2013

Statistical modeling of rare stochastic disturbance events at continental and global scales: post-fire debris flows and wildland fires

Karin Lynn Riley
The University of Montana

STATISTICAL MODELING OF RARE STOCHASTIC DISTURBANCE EVENTS AT CONTINENTAL AND GLOBAL SCALES: POST-FIRE DEBRIS FLOWS AND WILDLAND FIRES

By

KARIN LYNN RILEY

M.S. Environmental Systems, Humboldt State University, Arcata, California, USA, 2001

A.B. Earth and Planetary Science, Harvard and Radcliffe Universities, Cambridge, Massachusetts, USA, 1996

Dissertation

presented in partial fulfillment of the requirements
for the degree of

Doctor of Philosophy
in Geosciences

The University of Montana
Missoula, MT

December 2012

Approved by:

Sandy Ross, Associate Dean of the Graduate School
Graduate School

Rebecca Bendick, Co-Chair
Department of Geosciences

Anna E. Klene, Co-Chair
Department of Geography

Marc S. Hendrix
Department of Geosciences

Ulrich Kamp
Department of Geography

Emmanuel J. Gabet

Department of Geology, San Jose State University

Table of Contents

Abstract 1

Riley, Karin L., PhD in Geosciences, December 2012 Geosciences

Frequency-magnitude distribution of debris flows compiled from global data, and comparison with post-fire debris flows in the western U.S.

Rebecca Bendick and Anna E. Klene, Co-chairs

Forecasting debris flow hazard is challenging due to the episodic occurrence of debris flows in response to stochastic precipitation and, in some areas, wildfires. In order to facilitate hazard assessment, we have gathered available records of debris flow volumes into the first comprehensive global catalog of debris flows (n = 988). We also present results of field collection of recent debris flows (n = 77) in the northern Rocky Mountains, where debris flow frequency increases following wildfire. As a first step in parameterizing hazard models, we use frequency-magnitude distributions and empirical cumulative distribution functions (ECDFs) to compare volumes of post-fire debris flows to non-fire-related debris flows. The ECDF of post-fire debris flow volumes is significantly different (at 95% confidence) from that of non-fire-related debris flows, suggesting that the post-fire distribution is composed of a higher proportion of small events than that of non-fire-related debris flows. The slope of the frequency-magnitude distribution of post-fire debris flows is steeper than that of non-fire-related debris flows, corroborating evidence that small post-fire debris flows occur with higher relative frequency than non-fire-related debris flows. Taken together, the statistical analyses suggest that post-fire debris flows come from a different population than non-fire-related debris flows, and their hazard must be modeled separately. We propose two possible non-exclusive explanations for the fact that the post-fire environment produces a higher proportion of small debris flows: 1) following fires, smaller storms or effective drainage areas can trigger debris flows due to increased runoff and/or decreases in root strength, resulting in smaller volumes and increased probability of failure, 2) fire increases the probability and frequency of debris flows, causing their distribution to shift toward smaller events due to limitations in sediment supply.

Abstract 2

Riley, Karin L., PhD in Geosciences, December 2012 Geosciences

The relationship of large fire occurrence with drought and fire danger indices in the western US: the role of temporal scale

Rebecca Bendick and Anna E. Klene, Co-chairs

The relationship between large fire occurrence and drought has important implications for fire hazard prediction under current and future climate conditions. The primary objective of this study was to evaluate correlations between drought and fire-danger-rating indices representing short- and long-term drought, to determine which had the strongest relationships with large fire occurrence at the scale of the western United States during the years 1984-2008. We combined 4-8 km gridded drought and fire-danger-rating indices with information on fires greater than 1000 acres from the Monitoring Trends in Burn Severity project. Drought and fire danger indices analyzed were: monthly precipitation (PPT), Energy Release Component for fuel model G (ERC(G)), Palmer Drought Severity Index (PDSI), 3-month Standardized Precipitation Index (SPI3), SPI6 , SPI9, SPI12, and SPI24. To account for differences in indices across climate and vegetation assemblages, indices were converted to percentile conditions for each pixel, to indicate the relative anomaly in conditions during large fires. Across the western US, correlations between area burned and short-term indices ERC(G) and PPT percentile were strong (R^2 = 0.92 and 0.89 respectively), as were correlations between number of fires and these indices (R^2=0.94 and 0.93 respectively). As the period of time tabulated by the index lengthened, correlations between fire occurrence and indices weakened: PDSI and 24-month SPI percentile showed weak or negligible correlations with area burned (R^2 = 0.25 and -0.01 respectively) and number of large fires (R^2 = 0.3 and 0.01 respectively). This result suggests the utility of shorter-term rather than longer-term indices in fire danger applications. We attribute strong correlations between shorter-term indices and fire occurrence to strong associations between these indices and moisture content of dead fuels, which are the primary carriers of surface fire.

Acknowledgements

“It takes a village to complete a PhD.” That’s how the saying goes, isn’t it? If it isn’t, it should be. Karin Riley thanks her advisors, Rebecca Bendick and Anna Klene, for their guidance during her long and somewhat unconventional process. Completion of this degree would not have been possible without a generous Teaching Assistantship from the Department of Geosciences at the University of Montana that consistently paid the rent and bought sandwiches. Karin appreciates additional financial support from the Jerry O’Neal National Park Service Student Fellowship, a Geological Society of America Graduate Student Research Grant, a Bertha Morton Fellowship, and a Transboundary Research Award from the University of Montana. An army of fellow students and friends assisted with field work on steep talus slopes populated by wasps and bears. Last but not least, Karin is grateful for all the words of encouragement and hugs from her parents, Janet and Fred Riley, her partner Brian Elling, and friends, and support from her co-workers, especially Mark Finney, Kevin Hyde, and Faith Ann Heinsch.

Chapter 1.

Introduction

Statistical modeling of rare stochastic disturbance events presents a number of challenges. This dissertation investigates two disparate types of disturbance events: post-fire debris flows and large wildland fires. Debris flows and large fires are driven in part by stochastic events including lightning, wind events, and short-duration convective rainstorms. Because of their stochastic nature, it is often difficult to predict timing, location, or magnitude of these events. Due to their rarity, there are not sufficient records to predict wall-to-wall hazard or risk for an area solely using previous occurrences (Finney et al., 2011).

Despite the challenges mentioned above, prediction of these events is critically important, since debris flows and wildfires result in loss of human lives, as well as infrastructure including homes and roads (Cannon et al., 1998), These events also have direct or indirect effects on sediment transport (Wondzell and King, 2003), the water cycle, water quality, stream morphology (Hoffmann and Gabet, 2007), geomorphology of zero-order basins, transport of woody material to streams (Benda and Sias, 2003), habitat of threatened and endangered species, and carbon and nitrogen nutrient fluxes between vegetation, soil, water, and atmospheric pools (DeLuca and Sala, 2006; Riley et al., 2011). Thus, prediction of when and where fire and post-fire debris flow events will occur, and/or what magnitude they are likely to be, is of interest to a wide range of scientists, land managers, and residents of fire-prone ecosystems.

Input parameters for debris flow and wildfire hazard/risk vary widely from location to location, posing another challenge for researchers (Hungr et al., 2008; Finney et al., 2011). Hazard can be defined as either the consequence to a valued resource from a disturbance event or simply as the magnitude of the event (Hungr et al., 2008; Finney et al., 2011), while risk may be defined as the product of consequence and probability the event will occur.

Estimation of hazard and risk often requires records of event magnitudes for parameterization and accuracy assessment. Fairly comprehensive records of large wildland fires in the United States have existed for the past 20-30 years, but in order to parameterize statistical models of debris flows for a particular location, new data on debris flow extent and timing must usually be collected, a time-consuming and expensive endeavor (Hungr et al., 2008).

Obtaining other input data needed for parameterization of statistical and simulation models can also pose a challenge. Simulation models for wildfire occurrence incorporate predictors including weather, fuels, and topography (Finney et al., 2011). The relevance of these parameters may vary regionally (Littell et al., 2009). Statistical models predicting debris flow occurrence and magnitude have used factors including precipitation and slope thresholds, which vary locally, as well as basin morphology, lithology, and fire severity (Hyde et al., 2007; Gartner et al., 2008). While non-fire-related debris flows have been shown to follow a power-law frequency-magnitude distribution (van Steijn, 1996), the parameters of which can be used in predictive models, little was known about the distribution of post-fire debris flows when this research was undertaken.

This research sought to explain the variation in these two disparate and complex phenomena using simple unifying statistical models that worked across a range of coarse spatial scales (regional, continental, and global) regardless of lithology, climate, precipitation patterns, or vegetation assemblage. Such models have utility for broad hazard prediction at continental and global scales, and can illuminate physical mechanisms driving these disturbance phenomena. Another advantage is that such models minimize reliance on multiple input factors for which data may be difficult to obtain. Simple coarse-scale models are more readily related to other broad patterns, such as synoptic weather patterns or coupled sea-surface temperature and atmospheric teleconnections such as El Niño-Southern Oscillation or Pacific Decadal Oscillation, giving such models potential applications to long-lead forecasting and prediction of disturbances under climate change scenarios.

These studies are presented in this dissertation document in the form of two journal articles. Chapter 2 compares the empirical size distributions of post-fire and non-fire-related debris flows. This chapter was submitted to *Geomorphology* on June 2, 2012, and was subsequently revised based on the comments of reviewers and resubmitted on November 28, 2012, where it is in review as of this writing. Chapter 3 analyzes the relationship of drought with fire occurrence in the western US. This chapter was submitted to the *International Journal for Wildland Fire* in December 2011, and was revised and resubmitted on December 19, 2012.

In Chapter 2, the primary focus was to investigate the size distribution of debris flows. As a first step in parameterizing statistical hazard models, we used frequency-magnitude distributions and cumulative distribution functions to compare volumes of post-fire debris flows

to non-fire-related debris flows. A catalog of debris flow magnitudes from all over the world was compiled from a thorough literature review. Due to the large number of events required to parameterize frequency-magnitude distributions, and the relatively small number of post-fire event magnitudes recorded in the literature, field work was done to collect data on 73 recent post-fire events in the field. Field sites ranged from the Bitterroot Mountains of southwest Montana to the Smoky Mountains of Idaho. The resulting catalog of 988 debris flow has been accepted to the online data archive Pangaea, and is presented as a downloadable appendix to this document due to its large size (http://doi.pangaea.de/10.1594/PANGAEA.783654).

In Chapter 3, the main objective was to determine which, if any, drought and fire-danger-rating indices have the strongest relationship with large fire occurrence across the western United States during the years 1984-2008. Four-to-eight kilometer gridded drought and fire-danger-rating indices (monthly precipitation, Palmer Drought Severity Index, Standardized Precipitation Index, and daily Energy Release Component) were related to information on large fires (>1000 acres) from the Monitoring Trends in Burn Severity project (Eidenshink et al., 2007). To account for differences in indices across climate and vegetation assemblages, indices were converted to percentile conditions for each pixel, to indicate the relative anomalies in conditions during large fires.

In Chapter 4, the conclusions from each article were briefly reviewed, and accompanied by discussion of how these two disparate studies can be integrated to inform global and continental prediction of hazard and risk.

References

Benda, L., Sias, J., 2003. A quantitative framework for evaluating the wood budget. Journal of Forest Ecology and Management, 172, 1-16.

Cannon, S.H., Powers, P.S., Savage, W.Z., 1998. Fire-related hyperconcentrated and debris flows on Storm King Mountain, Glenwood Springs, Colorado, USA. Environmental Geology, 35(2-3), 210-218.

DeLuca, T.H., Sala, A., 2006. Frequent fire alters nitrogen transformations in ponderosa pine stands of the Inland Northwest. Ecology 87(10), 2511-2522.

Eidenshink, J.C., Schwind, B., Brewer, K., Zhu, Z.-L., Quayle, B., Howard, S., 2007. A project for monitoring trends in burn severity. Fire Ecology, 3(1), 3-21.

Finney, M.A., McHugh, C.W., Grenfell, I.C., Riley, K.L., Short, K.C., 2011. A simulation of probabilistic wildfire risk components for the continental United States. Stochastic Environmental Research and Risk Assessment, 25(7), 973-1000.

Gartner, J.H., Cannon, S.H., Santi, P.M., Dewolfe, V.G., 2008. Empirical models to predict the volumes of debris flows generated by recently burned basins in the Western U.S. Geomorphology, 96, 339-354.
Hoffmann, D.F., Gabet, E.J., 2007. Effects of sediment pulses on channel morphology in a gravel-bed river. GSA Bulletin, 119(1/2), 116-125.
Hungr, O., McDougall, S., Wise, M., Cullen, M., 2008. Magnitude-frequency relationships of debris flows and debris avalanches in relation to slope relief. Geomorphology, 96, 355-365.
Hyde, K., Woods, S.W., Donahue, J., 2007. Predicting gully rejuvenation after wildfire using remotely sensed burn severity data. Geomorphology, 86, 496-511.
Littell, J.S., McKenzie, D., Peterson, D.L., Westerling, A.L., 2009. Climate and wildfire area burned in western U.S. ecoprovinces, 1916-2003. Ecological Applications, 19(4), 1003-1021.
Riley, K.L., Ager, A., Finney, M.A., McMahon, A., 2011. Risk-based estimates of terrestrial carbon storage and wildfire emissions for the conterminous US, Association for Fire Ecology Interior West Fire Conference, Snowbird, Utah.
van Steijn, H., 1996. Debris-flow magnitude-frequency relationships for mountainous regions of Central and Northwest Europe. Geomorphology, 15, 259-273.
Wondzell, S.M., King, J.G., 2003. Postfire erosional processes in the Pacific Northwest and Rocky Mountain regions. Forest Ecology and Management, 178, 75-87.

Chapter 2.

Frequency-magnitude distribution of debris flows compiled from global data, and comparison with post-fire debris flows in the western U.S.

Karin L. Riley [a *], Rebecca Bendick [a], Kevin D. Hyde [b], and Emmanuel J. Gabet [c]

[a] Department of Geosciences, University of Montana, Missoula, Montana 59812, USA
[b] College of Forestry and Conservation, University of Montana, Missoula, Montana 59812, USA
[c] Department of Geology, San Jose State University, San Jose, California, 95192, USA
[*] Corresponding author. Tel. 1-406-329-4806, USA
*E-mail addres*s: karin.riley@umontana.edu

Keywords: debris flow; frequency; magnitude; fire

Words: Body: approximately 5,650. Abstract: 281

Abstract

Forecasting debris flow hazard is challenging due to the episodic occurrence of debris flows in response to stochastic precipitation and, in some areas, wildfires. In order to facilitate hazard assessment, we have gathered available records of debris flow volumes into the first comprehensive global catalog of debris flows (n = 988). We also present results of field collection of recent debris flows (n = 77) in the northern Rocky Mountains, where debris flow frequency increases following wildfire. As a first step in parameterizing hazard models, we use frequency-magnitude distributions and empirical cumulative distribution functions (ECDFs) to compare volumes of post-fire debris flows to non-fire-related debris flows. The ECDF of post-fire debris flow volumes is significantly different (at 95% confidence) from that of non-fire-related debris flows, suggesting that the post-fire distribution is composed of a higher proportion of small events than that of non-fire-related debris flows. The slope of the frequency-magnitude distribution of post-fire debris flows is steeper than that of non-fire-related debris flows, corroborating evidence that small post-fire debris flows occur with higher relative frequency than non-fire-related debris flows. Taken together, the statistical analyses suggest that post-fire debris flows come from a different population than non-fire-related debris flows, and their hazard must be modeled separately. We propose two possible non-exclusive explanations for the fact that the

post-fire environment produces a higher proportion of small debris flows: 1) following fires, smaller storms or effective drainage areas can trigger debris flows due to increased runoff and/or decreases in root strength, resulting in smaller volumes and increased probability of failure, 2) fire increases the probability and frequency of debris flows, causing their distribution to shift toward smaller events due to limitations in sediment supply.

Introduction

The majority of sediment transport in mountainous areas is caused by episodic events such as debris flows (Dietrich and Dunne, 1978; Kirchner et al., 2001). Debris flows move sediments ranging in size from mud to boulders several meters in diameter, and introduce them to stream channels, where this sudden influx of material can alter stream course and morphology (Costa, 1988; Benda et al., 2003; Ritter et al., 2006; Hoffmann and Gabet, 2007). When debris flows occur following wildfire events, they also transport burned tree trunks into streams, providing an additional source of topographic roughness as well as habitat for fish (Angermeier and Karr, 1984; Swanston, 1991; Brookes et al., 1996; Montgomery et al., 1996; Rieman and Clayton, 1997; Roghair et al., 2002; Benda and Sias, 2003). However, habitat may be negatively affected for 2-3 years after debris flows, and human populations are impacted when debris flows cross roads or collide with buildings (Lamberti et al., 1991; Rieman and Clayton, 1997; Cannon et al., 1998; Roghair et al., 2002). As the Wildland-Urban Interface in the Western US expands (Theobald and Romme, 2007), management of wildfire impacts to structures and roads, including damage from post-fire debris flows, has become an increasingly difficult issue. Prediction of debris flow events is desirable in order to mitigate short-term negative impacts and understand long-term benefits to habitat; however, prediction is difficult due to the stochastic nature of debris flow events.

Frequency-magnitude (FM) distributions quantify the relative probability of events of various sizes, and thus provide a means for evaluating stochastic natural hazards (Hungr et al., 2008; Finney et al., 2011; Thompson et al., 2011). Generally, small events occur exponentially more frequently than large events, and thus FM distributions for natural hazards often follow a power law, as has been demonstrated for earthquakes, landslides, and wildfires, as well as debris flows (Malamud and Turcotte, 1999; Helsen et al., 2002; Hungr et al., 2008; Jakob and Friele, 2010; Thompson et al., 2011). FM distributions have been used to parameterize local models for

debris flow hazard, but parameters vary from region to region, necessitating extensive data collection (Moon et al., 2005; Hungr et al., 2008; Conway et al., 2010; Jakob and Friele, 2010). Previous work on frequency-magnitude distributions has focused on non-fire-related debris flows, with the volume distribution of post-fire debris flows so far not addressed in the literature. As a first step toward creating universal models of debris flow hazards, we have compiled a global catalog of debris flow events in order to investigate similarities and differences between the populations of post-fire and non-fire-related debris flows.

The volume of a debris flow may be related to the process by which it initiates. Debris flows initiate through several mechanisms: 1) Landslides. During low-intensity long-duration storms, water infiltrates into the soil, causing elevated pore pressures; sediments that were close to their angle of repose while dry are likely to fail when saturated, thus increasing the probability of landslides (Ritter et al., 2006). Once a saturated parcel of soil fails, it can mobilize into a debris flow (Iverson et al., 1997). Landslide-initiated debris flows can start from shallow failures on the order of 1-2 cm where soils are hydrophobic (Gabet, 2003a) or from deeper failures measured in meters (Iverson et al., 1997; Wilkerson and Schmid, 2003; Stock and Dietrich, 2006; Jakob and Friele, 2010). Landslide-initiated debris flows often continue to entrain sediment as they move downslope, growing in volume (Hungr and Evans, 2004; Iverson et al., 2011; Mangeney, 2011). 2) Rockfall. Rockfall can be precipitated by earthquake, unstable slope angle (found in areas of deglaciation), or loss of vegetation (which commonly occurs following fire) (Jakob and Friele, 2010). When dry rocks fall into a channel that is carrying water, instantaneously increasing its sediment concentration, a debris flow can initiate. 3) Runoff. Infiltration-excess flow during high-intensity short-duration storms can produce rilling, entrainment of sediment, and gully rejuvenation through progressive sediment bulking, a process whereby sediment within the channel is mobilized until the fluid acquires a high enough solid component that interactions between particles affect the properties of the mixture and positive pore pressures are present (Iverson, 1997; Cannon et al., 1998; van Steijn, 1999; Cannon et al., 2001; Cannon et al., 2003; Conedera et al., 2003; Gabet and Mudd, 2006; Hyde et al., 2007; Gabet and Bookter, 2008; Santi et al., 2008; Jakob and Friele, 2010). 4) "Firehose effect". Sediments are mobilized by focused turbulent-water flows, often where water pours from a nickpoint or cliff (Helsen et al., 2002; Larsen et al., 2006; Conway et al., 2010). Although these mechanisms refer to separate triggering events, it is important to recognize that debris flows may

exhibit a combination of these different behaviors. For example, landslide-initiated debris flows often continue to entrain sediment as they move downslope, growing in volume (Hungr and Evans, 2004; Iverson et al., 2011; Mangeney, 2011). In addition, the generation of runoff in progressively bulked debris flows may initially be due to the failure of a thin layer of ash or soil on the order of 1-2 cm thick (Gabet, 2003a; Gabet and Sternberg, 2008).

Flow volume is also related to topographic relief and watershed area, with zero- and first-order watersheds with greater basin length or elevation change from ridge to valley potentially providing more material for entrainment by progressively bulked debris flows (Johnson et al., 1991; Hungr et al., 2008). Presence of side channels is also an important factor where debris flows are initiated by overland flow; Santi et al. (2008) found that side channels contributed material to debris flows in over half of the events they studied, with these contributions amounting to an average of 23% of the total volume.

The amount of sediment available for entrainment by debris flows is affected by the rate of sediment generation and erosion, which in turn is influenced by lithology and climate (Ritter et al., 2006). Time since last debris flow event is also an important factor, with more material becoming available as time since previous event increases (Jenkins et al., 2011). Time since previous debris flow event may be a more important factor in climate-limited systems (where sediment supply will be limited by the amount of time that has passed since the last event) than in transport-limited systems (where plenty of sediment is available, and becomes freed for transport by debris flows when vegetation is removed by fire).

Debris flow probability is related to a number of topographic factors, especially average slope (Gartner et al., 2008; Cannon et al., 2010). Precipitation amount, duration, and rate also influence debris flow probability and magnitude. In the case of runoff-initiated debris flows, precipitation amount and rate is related to the amount of infiltration-excess flow (Gartner et al., 2008). In most post-fire debris flow events in the Northern Rockies, the majority of material comes from hillslopes (Cannon et al., 2001) or gullies (Parrett et al., 2004; Santi et al., 2008) rather than soil-slip scars, so we expect that the location of rill and gully rejuvenation is important in determining debris flow volume, with more material available for entrainment if the debris flow initiates higher in the watershed. Higher precipitation amounts or rates also may increase the likelihood of the firehose effect, as well as the amount of material thus entrained. Longer precipitation durations increase the likelihood of mass failures caused by saturation

(Wondzell and King, 2003), but may not be directly related to debris flow volume, except where additional material is added through progressive sediment bulking in the gully (Hungr and Evans, 2004; Iverson et al., 2011; Mangeney, 2011).

High- and moderate-severity fire is strongly related to debris flow occurrence within zero- and first-order drainages (Hyde et al., 2007; Gartner et al., 2008; Cannon et al., 2010). In fire-dependent ecosystems, debris flow frequency is related to fire frequency, and may be responsible for driving Holocene aggradation through increases in erosion rates due to more frequent fire (Roering and Gerber, 2005). In Yellowstone, Pierce et al. (2004) found that debris flow magnitude and frequency were driven by climate and fire occurrence during the past 8000 years, with warmer climate being associated with severe droughts and stand-replacing fires in ponderosa pine forests (*Pinus ponderosa*), corresponding to large debris flow events. Cooler periods such as the Little Ice Age were associated with more frequent and less severe fire, and more frequent smaller debris flow events. Thus, climate effects on fire regime drive debris flow frequency and volume.

Fire increases the probability of debris flows through effects on soils and live and dead vegetation. Fire often changes the degree of soil repellency and its spatial pattern (Woods et al., 2007). Soil repellency can increase or decrease following fire (Prosser and Williams, 1998; Robichaud, 2000; Doerr et al., 2006; Doerr et al., 2009). The extent and connectivity of repellency affects infiltration of precipitation, and thus the amount of overland flow contributing to gully rejuvenation, but in general, patches of repellent soils are discontinuous, and infiltration is able to occur between them (Woods et al., 2007). Hyper-dry soil conditions following fire may entirely prevent infiltration during storm events (Moody and Ebel, 2012). Soil cohesion may decrease after fire due to loss of mycorrhizal associations and/or consumption of organic matter that binds soil aggregates, increasing post-fire sediment entrainment during precipitation events or through dry ravel (Spittler, 1995; Wondzell and King, 2003; Roering and Gerber, 2005). The presence of ash can decrease infiltration by clogging soil pores, especially in areas of coarser soils, and increase the transport capacity of runoff (Gabet and Sternberg, 2008; Woods and Balfour, 2010).

Fire severity is related to the extent of consumption of litter, duff, downed woody debris, and mortality of live vegetation (Prosser and Williams, 1998; Campbell et al., 2007). Live and dead vegetation intercepts precipitation, making it unavailable for overland flow, and impedes

dry ravel (Gabet, 2003b; Wondzell and King, 2003). When surface vegetation is removed by fire, dry ravel can accelerate: 2/3 of the total ravel occurring the year following a fire may occur during the first 24 hours (Bennett, 1982, as cited in Wondzell and King, 2003), rapidly filling gullies with material that can be mobilized by debris flows. Removal of vegetation increases incidence of raindrop splash on bare soil, which can mobilize sediment in the early stages of runoff-initiated debris flows, or cause surface sealing that promotes overland flow (Swanson, 1981; Meyer and Wells, 1997; Martin and Moody, 2001). Live vegetation contributes to the strength of mountainous slopes through root networks; when vegetation is killed by fire, roots decay over a period of years, causing a reduction in slope strength and reducing the resisting forces on a package of sediment, thus increasing the likelihood of landslide-initiated debris flows (Swanson, 1981; Meyer et al., 2001; Wondzell and King, 2003). Where debris flows are mobilized by landslides, loss of live vegetation can be a factor due to reduced evapotranspiration, which causes soils to remain wet over longer periods of time and thus decrease the amount of precipitation necessary for soil saturation (Swanson, 1981; Wondzell and King, 2003). However, most post-fire debris flows in the Rocky Mountain region appear to be mobilized by infiltration-excess flow, which is increased by the removal of live and dead vegetation.

Post-fire debris flow volume increases with areal extent of a zero-order basin burned by moderate- or high-severity fire (Gartner et al., 2008), due to removal of forest floor material, mycorrizae, and live vegetation, resulting in transport of more sediment by increased overland flow. Where vegetation is limited, debris flow occurrence is not influenced as heavily by fire (Larsen et al., 2006).

Timing of precipitation in relationship to fire events (and presumably other disturbances or land use change) strongly affects the amount of sediment delivery by debris flows (Lanini et al., 2009), as well as their probability (Wondzell and King, 2003). Following fire events, relatively small storm events can mobilize debris flows; Cannon (2008) found that a storms with less than 2-year recurrence interval were sufficient to generate debris flows in 25 recently burned watersheds in Colorado. Timing of precipitation event with regard to fire influences initiation mechanism as well. Debris flow events occurring approximately 0-5 years after a wildfire are likely to be runoff-initiated (prompted by increased overland flow due to fire effects on soil, and removal of live and dead vegetation), while events occurring approximately 5-10 years after fire are likely to be caused by saturation-induced slope failure (due to reduced root strength from

fire-induced vegetation mortality) (Meyer et al., 2001; Wondzell and King, 2003). These time periods vary with climate, which drives rates of vegetation regrowth.

Rather than attempt explicit prediction of debris flow volume and probability based on the above suite of factors, we statistically compared the size distributions and frequency-magnitude distributions of post-fire and non-fire-related debris flows, in order to establish similarities and differences. In order to have sufficient data for this task, we first assembled a catalog of debris flow magnitudes from the literature, and second, augmented this dataset with additional field collection.

Methods

Data acquisition

Catalog of previously researched events

Observations of individual debris flows were compiled into a global catalog from original field observations, unpublished raw observations from other researchers (Sue Cannon, Oldrich Hungr, and Dieter Rickenmann), and previously published studies (Sharp and Nobles, 1953; Doehring, 1968; Scott, 1971; Cleveland, 1973; Morton and Campbell, 1974; Klock and Helvey, 1976; Plafker and Ericksen, 1978; Fairchild and Wigmosta, 1983; Wells, 1987; Wieczorek et al., 1988; Cannon, 1989; Slosson et al., 1989; Pierson et al., 1990; Rickenmann and Zimmermann, 1993; Thurber Engineering and Golder Associates, 1993; McNeeley and Atkinson, 1996; DeGraff, 1997; Vallance and Scott, 1997; Booker, 1998; Cannon et al., 1998; Cenderelli and Kite, 1998; Iverson et al., 1998; van Steijn, 1999; Meyer et al., 2001; Helsen et al., 2002; Marchi et al., 2002; McDonald and Giraud, 2002; Clague et al., 2003; Conedera et al., 2003; Gartner et al., 2004; Gartner, 2005; Stock and Dietrich, 2006; Gabet and Bookter, 2008; Griswold and Iverson, 2008; Hungr et al., 2008; Santi et al., 2008; Conway et al., 2010; Stoffel, 2010).

In order to be included in this catalog, an estimate of the volume of material transported by the debris flow was required. Volume is the most common parameter chosen to represent magnitude of debris flows (van Steijn, 1996), and is directly related to the amount of material displaced by the event, as opposed to planimetric area, which may or may not be constrained by topography. Volume estimates were made using several different methods: 1) estimation from

the dimensions of the deposit, based on excavation, ground-penetrating radar, and/or GPS (as in some of our field measurements, as well as Cannon et al., 1998; Stock and Dietrich, 2006; Bothe, 2009; Jakob and Friele, 2010; Stoffel, 2010), 2) measurement of the amount of material displaced from gully by a series of cross-sections over the length of downcutting (Cannon, 1989; van Steijn, 1999; Gartner, 2005; Gabet and Bookter, 2008; Santi et al., 2008), 3) instrument measurement of flow velocity and cross-sectional area of channel (Marchi et al., 2002; Jakob and Friele, 2010), 4) estimates of scarp volume from aerial photos (Cannon, 1989), and 5) amount of material removed by cleanup crews (as in Cannon, personal communication). Each measurement method has associated error, but we were unable to estimate these errors in either sign or magnitude, and accepted the estimates of previous work as being the best available. Since most measurement methods were used in the samples of both post-fire and non-fire-related debris flows, their effect can be expected to be similar in both samples. Volume was the only required attribute for inclusion in the catalog, but we have included several additional attributes in the catalog when available (e.g. planimetric area of deposit, date of event, location, origin/cause, volume measurement method, the source of the debris flow information, whether the debris flow was post-fire, and the name of the associated fire event where applicable).

Field collection

While records of debris flows are rare, records of post-fire debris flows are even more sparse, with the volumes of only 97 events reported in the literature. Because FM distributions require a large number of events for parameterization, additional field collection of post-fire debris flow magnitudes was necessary for this study. We mapped debris flow fan inundation areas in recently burned areas in the Bitterroot, Sapphire, White Cloud, Smoky, and Sawtooth Mountains of Montana and Idaho (Figure 1). We visited sites as soon after the event as possible, a period which varied from as short as 3 months to as long as 8 years for events that occurred before this study was undertaken. At debris flow sites, we also collected data regarding initiation mechanisms (referenced in the catalog under the "Origin" field). Lithology of debris flow deposits varied by mountain range: in the Bitterroot and Smoky Mountains, primarily granite; in the Sapphires, primarily granite and metagranite; and in the Sawtooths, primarily porphyritic andesite and quartzite.

Field mapping employed kinematic GPS using a Trimble Juno SB. Specifically, we walked the perimeter of each deposit with the GPS unit in record mode. Perimeter files were corrected using the nearest base station. In order to check the fidelity of debris flow fan areas generated by this method, we selected a subset of four fans in Sleeping Child Creek, and measured these using a series of transects and a tape measure. Area estimates using the two methods were within 10% of each other, except in one case where the transect method missed a narrow lobe of the fan. Santi et al. (2008) cite the expected error when measuring debris flow volumes via GPS as -27% to + 37%, but our accuracy appeared to be much higher, perhaps due to improvements in GPS technology. We concluded that the kinematic GPS method was more accurate as well as more efficient than the transect method, and also had the advantage of producing georeferenced polygons which could be used in a GIS for further analysis.

For our field data, conversion of planimetric fan area to debris flow volumes followed Bothe (2009). The gravelly composition of the fans in Laird Creek permitted excavation of the fan material and direct location of the depth at which the new deposit was underlain by a thin organic horizon and older more weathered material. By digging in a number of locations interspersed on the fan, Bothe (2009) produced a mean estimate of depth for five of the fans in Laird Creek where we collected perimeter data; planimetric areas of each fan were multiplied by the mean depth estimate for that fan to produce volume estimates. These average depth estimates ranged from 0.14 – 0.34 m, with a watershed mean of 0.24 m. For fans in Laird Creek that lacked a direct measurement, the mean depth estimate of 0.24 m was used to produce volume estimates. This coefficient was also used for similar deposits in Warm Springs Creek (fan deposits consisted of primarily gravelly material and were generally not constrained by topography). In Sleeping Child Creek, digging was not possible due to the prevalence of cobble and boulder-sized clasts in the fan deposits, and deposits appeared to be thicker, perhaps due to a more viscous slurry and/or confinement by the narrow valley. Here, we used linear regression of our planimetric area measurements against lower-bound volume estimates produced by measurements of gully morphology by Gabet and Bookter (2008) for the same gullies (m = 0.6, n = 6, R^2 = 0.55). The lower-bound estimate was chosen since it is likely that some material was lost into Sleeping Child Creek during the debris flow event, meaning the fan deposit is smaller than the material displaced from the gully. For deposits in Sleeping Child Creek, planimetric area was thus multiplied by 0.6 m to produce a volume estimate. Notably, this coefficient is almost

identical to that produced by linear regression of area and volume figures presented by Cannon et al. (1998) for debris flows following a fire on Storm King Mountain in Colorado. This coefficient was also applied to debris flow fan areas in Rooks Creek, Fourth of July Creek, Rye Creek, Two Bear Creek, and the Sawtooths, where the clast size distribution of the deposits was similar to that of Sleeping Child Creek and/or debris flows tended to be constrained by narrow valley topography.

Comparing our estimates of volume derived by direct measurements of thickness and area for five debris flows in Laird Creek with volume estimates derived from our model using 0.24 m thickness, errors varied from as low as 1 m^3 to as high as 641 m^3 (1% to 79%). We expect similar error rates where this model was used, in the remainder of Laird Creek and Warm Springs Creek, with an additional up to 10% estimated error resulting from kinematic GPS measurements of areas. Error rates are difficult to estimate for the other watersheds, where we were not able to collect direct measurements of debris flow thickness. Such uncertainty in volume measurements does not affect FM distributions greatly, since measurements are grouped into bins; for this study, bin sizes were 10,000 m^3, and multiplying most debris flow volumes collected for this study by +/-79% would not change the subsequent bin assignment, since most volumes are less than 300 m^3. In addition, unless this method systematically over- or under-estimated volumes, the net effect of error on the slope of the FM distribution would be small.

Statistical methods

In order to compare the distribution of post-fire debris flow volumes with that of non-fire-related debris flows, we divided events into two categories: those that occurred in recently-burned areas and those that did not. Volume data was explored graphically, using boxplots and regional groupings.

For both categories, debris flow frequency-magnitude distributions were compiled from the catalog. Robust regression was performed on the data in log-log space, using the Kendall's Tau statistic, which is more robust to outliers than traditional linear regression methods and does not assume normality of residuals (Sen, 1968). We used the median volume for each frequency as the dependent variable as in Finney et al. (2011), which reduced the disproportionate effect of the rarest largest events on the slope coefficient, and produced a better fit with more frequently

occurring event sizes. The slope parameter quantifies the ratio of small to large debris flows (Finney et al., 2011), and thus is the parameter of interest in this project. The intercept parameter is of little interest in this study, since it is strongly influenced by sample size; larger y values are generated by larger sample sizes. To evaluate the similarity of the slope parameter of the post-fire debris flow frequency-magnitude distribution to that of non-fire-related debris flows, we calculated a 95% confidence interval around the slope parameters.

In addition, the empirical cumulative distribution functions (ECDFs) of volume for post-fire and non-fire-related debris flows were compared. We computed the nonparametric test statistic D, the maximum separation distance between the two distributions. As D increases, so does the likelihood that the two distributions are different. The Kolmogorov-Smirnov test was used to determine the likelihood that the ECDF of post-fire debris flows is different than that of non-fire-related debris flows, based upon D.

Results

Field collection

In the field, we collected volume measurements of recent debris flows in 77 zero-order drainages at the sites shown in Figure 1 and Table 1. Of these debris flows, only three were not related to wildfires. Debris flows occurred in clusters in several watersheds; these clusters appear to be due to the conjunction of two events: a wildfire of moderate to high severity and a localized rainstorm. The upper third of zero-order watersheds that produced debris flows generally had experienced high tree mortality following wildfire, likely resulting in increased overland flow during storms. From observations of rejuvenated rill networks and available rainfall records, we determined that all 74 post-fire debris flow events were initiated by intense precipitation within 1-2 years of a wildfire, which led to overland flow, rilling, and mobilization of material in the gully, in other words, runoff initiation. Physical evidence for runoff initiation consisted of a sudden transition from rill to a gully head with abrupt downcutting, as well as the absence of a discrete scarp (Figure 2). Data were insufficient to reconstruct rainfall that initiated some debris flows, but where precipitation data were available from a nearby station, recurrence intervals for storms related to these debris flows had a less than 2- to 25-year recurrence interval (Parrett et al., 2004).

Recent deposits are visibly less weathered than the paleofan, and lack lichen and vegetative cover. It is possible that several recent debris flows have occurred in an individual gully, and are superposed. We were not able to differentiate multiple recent debris flow deposits from pulses within a single debris flow, and found evidence of multiple surges in the form of lobes perched atop the main deposit. At Sleeping Child Creek, we concluded that in some cases tributary gullies failed after the main gully, but during the same storm. It was not possible, however, to determine whether the time interval between failures was seconds, minutes, or hours. Superposition of recent debris flow deposits is a potential source of error in the catalog as a whole. It is uncertain whether errors of this type would occur with the same frequency in the post-fire and non-fire-related populations. We assume here that each recent deposit was generated during a single storm. The combined volume at the end of the storm is arguably the best estimation of hazard and impact to highly valued resources, and might still be considered a single "event" since it was generated during a single storm.

A debris flow site typical of our study area is shown in Figure 3: a rejuvenated gully leading to a poorly-sorted non-stratified deposit, often with levees present. Deposits consisted of a sandy matrix, with clasts ranging from sand to cobble or boulder (Figure 4). Some valley floors, such as Rye Creek of the Sapphire Mountains and nearby Laird Creek in the southern Bitterroot Mountains, are formed entirely from a sequence of alternating debris flow fans and paleofans (Figure 5).

Statistical analyses of debris flow volumes in catalog

The 77 debris flows measured during this study were combined with those from the literature to form a catalog of 988 events. The catalog can be accessed through Pangaea at http://doi.pangaea.de/10.1594/PANGAEA.783654. Figure 6 shows the geographical distribution of debris flows by nation. Canada, France, Switzerland, and the USA are the only nations to have over 50 records of debris flow volumes. No records are present in the catalog for Asia, Africa, or Australia, which of course does not suggest that these areas do not experience debris flows, only that no debris flow volume data have been published in the scientific literature. Even with our effort to augment the sample of post-fire debris flows via field collection, it was smaller than that of non-fire-related debris flows (n = 264 vs. n = 724). Given the limitations of this dataset,

statistical analyses in this manuscript must therefore be considered a first step toward hazard and risk modeling of debris flows, and understanding of differences and similarities in the size distributions of post-fire and non-fire-related debris flows.

Debris flow volumes in the catalog spanned 10 orders of magnitude. Volumes in the same region are generally more similar to one another than to volumes at other locations, but volumes vary as much as four orders of magnitude even within the same location (Table 2; Figure 7). This regional similarity may be a result of the topography (e.g. difference in elevation from ridge to valley floor, slope, and/or basin length), geology, disturbance history (e.g. fire-prone versus non-fire-prone ecosystem), and/or climate (e.g. size of the characteristic storm of the area, temperature ranges). The Wasatch is the only region with a number of both post-fire and non-fire-related debris flows recorded, and there the median post-fire debris flow is larger than the median non-fire-related debris flow. However, we lack information on basin geometry, storm rainfall that precipitated these debris flows, geology, etc. at these Wasatch sites, and cannot attribute this difference to recent burning.

The global size distributions of post-fire debris flows and non-fire-related debris flows showed some notable differences. The median volume of post-fire debris flows was smaller than that of non-fire-related debris flows, with the largest non-fire-related debris flow in the catalog being three orders of magnitude larger than the largest post-fire debris flow (Figure 8, Table 3). To test whether the lack of large events among post-fire debris flows could be a result of the smaller sample size, since large events are extremely rare, we took a random sample from the non-fire-related debris flows of the number as the post-fire debris flow sample (n = 264), and compared the size of the largest events. In 98 of 100 samples, the largest non-fire-related debris flow was still larger than the largest post-fire debris flow, suggesting that catalog completeness is not the source of differences in the size distribution.

The slope of the frequency-magnitude distribution of post-fire debris flows is steeper than that of non-fire-related debris flows (Figure 9, Table 3). The 95% confidence intervals around the two slope parameters do not overlap, signifying that the two parameters are significantly different (Figure 10), and meaning that the ratio of large to small debris flows is different for the two categories, with a higher proportion of small events occurring in the post-fire debris flow sample.

Another method for comparing two distributions is to plot the empirical cumulative distribution functions (ECDFs). The ECDF of post-fire debris flows generally plots to the left of the ECDF of non-fire-related debris flows (Figure 11), signifying that post-fire debris flows tend to consist of more smaller volumes. The maximum separation between the two distributions, or D, was equal to 0.1. The Kolmogorov-Smirnov test was used to test the hypothesis that post-fire debris flows tend to be smaller, yielding a p-value of 0.02 – meaning that the likelihood of a separation distance that large or larger occurring by chance in a random sample if indeed the two distributions are from the same population is approximately 1 in 50. This result constitutes strong evidence that the distribution of post-fire debris flow volumes is composed of smaller values than that of non-fire-related debris flows.

Initiation mechanism was reported for 422 debris flows in the catalog, or 43%. Of those debris flows, runoff is the most common initiation mechanism for both non-fire-related (n = 199, or 63%) and post-fire debris flows (n = 90, or 87%). Landslides are the second most common initiation mechanism in both groups, with 90 non-fire-related debris flows (28%) and 14 post-fire events (13%) initiating this way. Of non-fire related debris flows, 15 (5%) are known to have initiated through the firehose effect and 14 (4%) through rockfall. This result is consistent with previous studies, which observed that the most prevalent initiation mechanism for post-fire debris flows in the U.S. Interior West is runoff (Spittler, 1995; Hyde et al., 2007; Santi et al., 2008).

Runoff-initiated debris flows tended to be larger and less variable in volume than those initiating through landslides (Figure 12). The median volume of runoff-initiated debris flows was 1951 m^3, in contrast to 279 m^3 for those that initiated through landslides. The largest volumes for runoff-initiated debris flows were recorded by van Steijn (1999) in the French Alps (n = 198); debris flows in the Alps tend to have larger volumes than most other areas (Figure 7). When runoff-initiated debris flows are further grouped into post-fire and non-fire-related events, post-fire events are smaller (Figure 13). These results demonstrate that initiating mechanism is not driving the differences in volumes between post-fire and non-fire-related samples.

In summary, these statistical analyses indicate differences in magnitudes of post-fire and non-fire-related debris flows, independent of initiation mechanism. The ECDF of volumes of post-fire debris flows differs from that of non-fire-related debris flows, as does the slope of the FM distribution, indicating that small debris flows occur more frequently in the post-fire sample.

Discussion

Two major contributions of this manuscript are: 1) compilation of the first global catalog of debris flows, and 2) statistical analyses suggesting that the size distributions of post-fire and non-fire-related debris flows are different. However, these efforts constitute only a first step toward hazard and risk modeling at global scales due to the low number of debris flow volumes published in the literature and lack of attribute data on many important drivers of debris flow volume (e.g. topography, climate, weather, and geology). We see an analogy between debris flow and earthquake catalogs. Prior to the 1950s, the seismograph network was small; correspondingly, records of earthquakes were relatively few, and it was thus difficult to characterize earthquake risk. For the past several decades, the seismograph network has been extensive enough to capture all earthquakes globally, resulting in sufficient records to parameterize the frequency-magnitude distribution of earthquakes at the global scale. The state of the current debris flow catalog is not dissimilar to that of earthquakes in the 1950s.

Despite the small number of records of debris flow magnitudes, it is evident that moderate- and high-severity wildfire increases the probability of debris flows by increasing their frequency through a suite of changes in vegetation, soil characteristics, and sediment supply. By removing vegetation, adding ash, and producing changes in the soil surface, fires decrease the stability of zero-order watershed systems and make them more prone to debris flow activity. As evidence, we rely on our field observations as well as previous research demonstrating that relatively small storms (e.g. with a 2-year return interval (Parrett et al., 2004; Cannon et al., 2010)) can provoke debris flows in recently burned basins while nearby unburned basins do not experience debris flow activity.

However, post-fire debris flows tend to be smaller. We expect that in most fire-prone environments, sediment transport is supply-limited. Once fire removes vegetation, dry ravel can dramatically accelerate, moving material into gullies, where it can be mobilized by overland flow when a storm occurs (Bennett, 1982, as cited in Wondzell and King, 2003). Sediments that were stable when retained by live and dead vegetation now roll downhill under the influence of gravity (Gabet 2003b). Once in the gully, gravel, cobbles, and boulders can be mobilized by a slurry of overland flow during fairly short-return-interval (~2 yrs) storms. Once the gully is

empty and sediments have been mobilized, repeat debris flows at the same site are unlikely in the short term (unless additional side channels fail during future storms).

This change in frequency and magnitude relations in the post-fire regime can be attributed to either or both of the two components prerequisite to the generation of runoff-initiated debris flows: overland flow and fine-grained sediment. Both components increase in the post-fire environment. More overland flow occurs during intense storms due to: 1) decreased rainfall interception by vegetation, resulting from mortality of the overstory and consumption of live and dead vegetation by fire, with removal of vegetation increasing with fire severity (Wondzell and King, 2003; Campbell et al., 2007; Parise and Cannon, 2012); 2) surface roughness may decrease due to consumption of litter and duff layers, removing impediments to runoff (Lavee et al., 1995); 3) where ash overlays coarse soils, infiltration is reduced due to the small grain size of the ash particles (Gabet and Sternberg, 2008; Woods and Balfour, 2010; Gabet and Bookter, 2011); and 4) extent of hydrophobic soil and/or hyperdryness sometimes increase following fires, although their spatial pattern is generally discontinuous enough to allow infiltration (Woods et al., 2007; Moody and Ebel, 2012). Availability of fine-grained sediments increases following fire due to several factors: 1) vegetation has been converted to ash, which is abundant following high-severity fire (Gabet and Sternberg, 2008); 2) consumption of litter and duff exposes underlying soil; and 3) fire can break down soil aggregates (Spittler, 1995; Wondzell and King, 2003; Roering and Gerber, 2005); 4) pH of debris flow fluid can be increased by ash, which can cause dispersion of clay compounds and thus facilitate their entrainment (Gabet and Bookter, 2011). In addition, the bulk density and viscosity of runoff can be increased by the incorporation of ash (Burns, 2007; Gabet and Sternberg, 2008), which enables it to entrain more sediment and prevents positive pore pressures from dissipating. These changes allow runoff-initiated post-fire debris flows to occur in smaller zero-order drainages during smaller precipitation events than in unburned environments, increasing the proportion of small debris flows following fires.

Changes in the post-fire environment also increase initiation of debris flows by landsliding in some areas, due to increased soil saturation and decreased strength of regolith. owever, these factors also apply to debris flow initiation by landslides. Soil saturation during long-duration low-intensity storms can increase following fires, especially those of moderate/high severity due to: 1) mortality of trees, shrubs, and herbaceous plants leads to

decreased evapotranspiration, increasing soil moisture and decreasing the amount of infiltration necessary for saturation (Swanson, 1981; Wondzell and King, 2003); and 2) interception by canopy, understory, litter and duff layers is reduced (Dunne and Leopold, 1978 as cited in Gabet and Sternberg, 2008), making more water available for infiltration. A second factor is that the strength of the regolith is reduced due to vegetation mortality, causing a loss of root strength. We hypothesize that because debris flows can occur in response to smaller perturbations (e.g. smaller storms) due to changes in the post-fire environment or in smaller hollows where elevated subsurface flow is concentrated, the frequency of small debris flows increases after fires.

In the catalog as well as our field research, all post-fire debris flows in the U.S. Interior West were initiated by runoff within 0-5 years of fire, while post-fire debris flows near the U.S. West Coast initiated by either landslides or runoff. This pattern is likely due to characteristics of precipitation: in the Interior West, summer convective storms are common, and can generate high enough precipitation rates to produce overland flow (Wondzell and King, 2003). Summer convective storms can occur near the West Coast as well. Long-duration low-intensity storms that can produce saturation-induced debris flows are not common in the Interior West, however, but do occur on the West Coast.

The level and patterning of fire severity within a watershed adds a source of variability to the magnitude of debris flows generated therein. For most post-fire debris flows in the Northern Rockies, the majority of material comes from rilling of hillslopes (Cannon et al., 2001) or gullies (Parrett et al., 2004; Santi et al., 2008), rather than soil-slip scars, so we expect that the location of rill and gully rejuvenation is important in determining debris flow volume, with more material available for entrainment if the debris flow initiates higher in the watershed. Where more material is removed in the upper reaches of a catchment by high severity fire, we expect that gully rejuvenation will occur higher in the watershed, increasing the runout length, and the amount of material entrained.

This study entails large formal and informal uncertainties driven largely by the small sample size. We do not expect that uncertainty in debris flow volume estimation significantly affects our results, however, since FM distributions are fairly robust to such uncertainty, due to binning of observations. Augmentation of the catalog will require further data collection or cooperation of additional researchers. While literature review supports the conclusion that this catalog is currently the most complete record of debris flow magnitudes, it is only marginally

sufficient for parameterizing FM distributions. For example, if we omit debris flows that followed the Station Fire (n = 94) from our analysis, then the confidence intervals of the slope parameters of the two FM distributions overlap. Given the limited sample size and the lack of attribute data on topography, precipitation, time since last debris flow, sediment generation rates, and fire severity, we could not examine the interaction of these driving factors in producing predictions of debris flow volume. We also noted that some geographic areas were better-represented than others in our catalog; despite efforts to contact researchers, we were not able to obtain data for debris flows in Asia, Australia, or Africa. Some geographic areas were represented only by post-fire or non-fire-related debris flows, but not both, e.g. all debris flows except three in the Rockies and Southern California are post-fire, while all debris flows in Hawaii, British Columbia, and the Alps are non-fire-related (with the exception of one post-fire debris flow recorded by Conedera et al. (2003)).

Despite inherent error and challenges presented by small sample sizes, the catalog and associated statistical analyses provide a first step in global hazard modeling of debris flows. As a possible starting point for future research, we propose two alternate and non-exclusive hypotheses to explain why post-fire debris flows tend to be smaller than non-fire-related debris flows. First, smaller storms or effective drainage areas can trigger debris flows because of increases in the generation of overland flow, in the case of runoff-initiated debris flows, or decreases in root cohesion, in the case of landslide-initiated debris flows. These changes result in a higher probability of failure and smaller debris flow volumes. Second, debris flow volumes in most environments are limited by the supply of available loose material; we expect that fire increases the probability and frequency of debris flows, causing post-fire debris flows to be smaller because less sediment is available in each event.

Conclusions

Based on our catalog of 988 events, post-fire debris flows tend to be smaller than non-fire-related debris flows. For post-fire debris flows, the slope of the frequency-magnitude distribution is steeper, meaning that the ratio of small to large events is higher than in unburned areas, indicating that small debris flows occur with higher proportional frequency. Fire produces a number of changes in vegetation and soil characteristics that increase overland flow, available

sediment, and soil moisture, as well as decreasing the strength of the regolith; we propose that these changes increase the proportional frequency of small debris flows, and produce debris flows in small zero-order drainages not susceptible to debris flows under unburned conditions. In regions where sediment transport is supply-limited, wildfire provokes smaller debris flows by increasing their probability and frequency. Models for hazard prediction of post-fire debris flows therefore should be parameterized separately from non-fire-related debris flows, and will likely include different predictor variables.

Acknowledgements

This study was funded in part by a Geological Society of America Graduate Student Research Grant and a University of Montana Transboundary Research Award to Karin Riley. This work was also funded in part by the U.S. Forest Service's Rocky Mountain Research Station and Western Wildland Environmental Threat Center. We are grateful for intrepid off-trail field help at the mercy of wasps and bears, from Davis Bothe, Esther Bowlin, Brian Elling, Dan Hoffmann, Morgan Hyde, Chuck Irestone, Jack Kehoe, Solmaz Mohadjer, and Warren Roe. We appreciate collaboration with Sue Cannon, Anna Klene, and Henk van Steijn throughout this project, as well as constructive review of this manuscript by Isaac Grenfell. Sue Cannon, Oldrich Hungr, Dieter Rickenmann, and Henk van Steijn generously provided extensive unpublished datasets that are included in the catalog.

References

Angermeier, P.L., Karr, J.R., 1984. Relationships between woody debris and fish habitat in a small warmwater stream. Transactions of the American Fisheries Society, 113(6), 716-726.

Benda, L., Miller, D., Bigelow, P., Andras, K., 2003. Effects of post-wildfire erosion on channel environments, Boise River, Idaho. Forest Ecology and Management, 178, 105-119.

Benda, L., Sias, J., 2003. A quantitative framework for evaluating the wood budget. Journal of Forest Ecology and Management, 172, 1-16.

Bennett, K.A., 1982. Effects of slash burning on surface erosion rates in the Oregon Coast Range. Master's Thesis, Oregon State University, Corvallis, Oregon, 70 pp.

Booker, F.A., 1998. Landscape and management response to wildfires in California, University of California, Berkeley, 436 pp.

Bothe, D., 2009. Area-to-volume relationships of debris flow deposits in the Rocky Mountains of western Montana, USA. Senior Thesis, University of Montana, Missoula, Montana, 33 pp.

Brookes, A., Knight, S.S., Shields Jr., F.D., 1996. Chapter 4: Habitat Enhancement. In: A. Brookes, F.D. Shields Jr. (Eds.), River channel restoration: guiding principles for sustainable projects. John Wiley and Sons Ltd., Chichester, pp. 103-126.

Burns, K.A., 2007. The effective viscosity of ash-laden flows. Master's Thesis, University of Montana, Missoula, Montana, 107 pp.

Campbell, J., Donato, D., Azuma, D., Law, B., 2007. Pyrogenic carbon emissions from a large wildfire in Oregon, United States. Journal of Geophysical Research, 112, G04014.

Cannon, S.H., 1989. An evaluation of the travel-distance potential of debris flows. Utah Geological and Mineral Survey Miscellaneous Publication 89-2 35 pp.

Cannon, S.H., Gartner, J.E., Parrett, C., Parise, M., 2003. Wildfire-related debris-flow generation through episodic progressive sediment-bulking processes, western USA. In: D. Rickenmann, Chen (Eds.), Debris-flow hazards mitigation: mechanics, prediction, and assessment. Millpress, Rotterdam.

Cannon, S.H., Gartner, J.E., Rupert, M.G., Michael, J.A., Rea, A.H., Parrett, C., 2010. Predicting the probability and volume of postwildfire debris flows in the intermountain western United States. GSA Bulletin, 122(1/2), 127-144.

Cannon, S.H., Gartner, J.E., Wilson, R.C., Bowers, J.C., Laber, J.L., 2008. Storm rainfall conditions for floods and debris flows from recently burned areas in southwestern Colorado and southern California. Geomorphology, 96(3-4), 250-269.

Cannon, S.H., Kirkham, R.M., Parise, M., 2001. Wildfire-related debris-flow initiation processes, Storm King Mountain, Colorado. Geomorphology, 39, 171-188.

Cannon, S.H., Powers, P.S., Savage, W.Z., 1998. Fire-related hyperconcentrated and debris flows on Storm King Mountain, Glenwood Springs, Colorado, USA. Environmental Geology, 35(2-3), 210-218.

Cenderelli, D.A., Kite, J.S., 1998. Geomorphic effects of large debris flows on channel morphology at North Fork Mountain, eastern West Virginia, USA. Earth Surface Processes and Landforms, 23, 1-19.

Clague, J.J., Friele, P.A., Hutchinson, I., 2003. Chronology and hazards of large debris flows in the Cheekye River basin, British Columbia, Canada. Environmental and Engineering Geoscience, 8, 75-91.

Cleveland, G.B., 1973. Fire and rain = mudflows, Big Sur, 1972. California Geology, 26, 127-135.

Conedera, M., Peter, L., Marxer, P., Forster, F., Rickenmann, D., Re, L., 2003. Consequences of forest fires on the hydrogeological response of mountain catchments: a case study of the Riale Buffaga, Ticino, Switzerland. Earth Surface Processes and Landforms, 28, 117-129.

Conway, S.J., Decaulne, A., Balme, M.R., Murray, J.B., Towner, M.C., 2010. A new approach to estimating hazard posed by debris flows in the Westfjords of Iceland. Geomorphology, 114, 556-572.

Costa, J.E., 1988. Rheologic, geomorphic, and sedimentologic differentiation of water floods, hyperconcentrated flows, and debris flows. In: V.R. Baker, R.C. Kochel, P.C. Patton (Eds.), Flood geomorphology. John Wiley & Sons, New York, pp. 113-122.

DeGraff, J.V., 1997. Geologic investigation of the Pilot Ridge debris flow, Groveland Ranger District, Stanislaus National Forest. USDA Forest Service 20 pp.

Dietrich, W.E., Dunne, T., 1978. Sediment budget for a small catchment in mountainous terrain. Zeitschrift fur Geomorphologie Supplement Bd. 29, 191-206.

Doehring, D.O., 1968. The effect of fire on geomorphic processes in the San Gabriel Mountains, California. In: R.B. Parker (Ed.), Contributions to Geology. University of Wyoming, Laramie, WY, pp. 43-65.

Doerr, S.H., Shakesby, R.A., Blake, W.H., Chafer, C.J., Humphreys, G.S., Wallbrink, P.J., 2006. Effects of differing wildfire severities on soil wettability and implications for hydrological response. Journal of Hydrology, 319, 295-311.

Doerr, S.H., Shakesby, R.A., MacDonald, L.H., 2009. Soil water repellency: a key factor in post-fire erosion? In: A. Cerda, P.R. Robichaud (Eds.), Fire effects on soils and restoration strategies: land reconstruction and management. Science Publishers, Enfield, NH, pp. 197-223.

Dunne, T., Leopold, L.B., 1978. Water in environmental planning. W.H. Freeman & Co., San Francisco, 818 pp.

Fairchild, L.H., Wigmosta, M., 1983. Dynamic and volumetric characteristics of the 18 May 1980 lahars on the Toutle River, Washington, Proceedings of the Symposium on Erosion Control in Volcanic Areas Tech. Mem. 1908. Japan Public Works Research Institute Ministry of Construction, Tokyo, pp. 131-153.

Finney, M.A., McHugh, C.W., Grenfell, I.C., Riley, K.L., Short, K.C., 2011. A simulation of probabilistic wildfire risk components for the continental United States. Stochastic Environmental Research and Risk Assessment, 25(7), 973-1000.

Gabet, E.J., 2003a. Post-fire thin debris flows: sediment transport and numerical modelling. Earth Surface Processes and Landforms, 38, 1341-1348.

Gabet, E.J., 2003b. Sediment transport by dry ravel. Journal of Geophysical Research, 108(B1), doi:10.1029/2001JB001686.

Gabet, E.J., Bookter, A., 2008. A morphometric analysis of gullies scoured by post-fire progressively bulked debris flows in southwestern Montana, USA. Geomorphology, 96, 298-309.

Gabet, E.J., Bookter, A., 2011. Physical, chemical and hydrological properties of Ponderosa pine ash. International Journal of Wildland Fire, 20, 443-452.

Gabet, E.J., Mudd, S.M., 2006. The mobilization of debris flows from shallow landslides. Geomorphology, 74, 207-218.
Gabet, E.J., Sternberg, P., 2008. The effects of vegetative ash on infiltration capacity, sediment transport, and the generation of progressively bulked debris flows. Geomorphology, 101(4), 666-673.
Gartner, J.E., 2005. Relations between wildfire related debris-flow volumes and basin morphology, burn severity, material properties and triggering storm rainfall, University of Colorado, 87 pp.
Gartner, J.E., Bigio, E.R., Cannon, S.H., 2004. Compilation of post wildfire runoff-event data from the Western United States. U.S. Geological Society Open-File Report 2004-1085, accessed online at http://pubs.usgs.gov/of/2004/1085/ofr-04-1085.html on January 2, 2012.
Gartner, J.H., Cannon, S.H., Santi, P.M., Dewolfe, V.G., 2008. Empirical models to predict the volumes of debris flows generated by recently burned basins in the Western U.S. Geomorphology, 96, 339-354.
Griswold, J.P., Iverson, R.M., 2008. Mobility statistics and automated hazard mapping for debris flows and rock avalanches. U.S. Geological Survey: Reston, VA. Scientific Investigations Report 2007-5276, 59 pp.
Helsen, M.M., Koop, P.J.M., Van Steijn, H., 2002. Magnitude-frequency relationship for debris flows on the fan of the Chalance Torrent, Valgaudemar (French Alps). Earth Surface Processes and Landforms, 27, 1299-1307.
Hoffmann, D.F., Gabet, E.J., 2007. Effects of sediment pulses on channel morphology in a gravel-bed river. GSA Bulletin, 119(1/2), 116-125.
Hungr, O., Evans, S.G., 2004. Entrainment of debris in rock avalanches: an analysis of a long run-out mechanism. Geological Society of America Bulletin, 116(9/10), 1240-1252.
Hungr, O., McDougall, S., Wise, M., Cullen, M., 2008. Magnitude-frequency relationships of debris flows and debris avalanches in relation to slope relief. Geomorphology, 96, 355-365.
Hyde, K., Woods, S.W., Donahue, J., 2007. Predicting gully rejuvenation after wildfire using remotely sensed burn severity data. Geomorphology, 86, 496-511.
Iverson, R.M., 1997. The physics of debris flows. Reviews of Geophysics, 35(3), 245-296.
Iverson, R.M., Reid, M.E., LaHusen, R.G., 1997. Debris-flow mobilization from landslides. Annual Review of Earth and Planetary Sciences, 25, 85-138.
Iverson, R.M., Reid, M.E., Logan, M., LaHusen, R.G., Godt, J.W., Griswold, J.P., 2011. Positive feedback and momentum growth during debris-flow entrainment of wet bed sediment. Nature Geoscience, 4, 116-121.
Iverson, R.M., Schilling, S.P., Vallance, J.W., 1998. Objective delineation of lahar-inundation hazard zones. Geological Society of America Bulletin, 110(8), 972-984.
Jakob, M., Friele, P., 2010. Frequency and magnitude of debris flows on Cheekye River, British Columbia. Geomorphology, 114, 382-395.
Jenkins, S.E., Sieg, C.H., Anderson, D.E., Kaufman, D.S., Pearthree, P.A., 2011. Late Holocene geomorphic record of fire in ponderosa pine and mixed-conifer forests, Kendrick Mountain, northern Arizona, USA. International Journal of Wildland Fire, 20, 125-141.
Johnson, P.A., McCuen, R.H., Hromadka, T.V., 1991. Magnitude and frequency of debris flows. Journal of Hydrology, 123, 69-82.

Kirchner, J.W., Finkel, R.C., Riebe, C.S., Granger, D.E., Clayton, J.L., King, J.G., Megahan, W.F., 2001. Mountain erosion over 10 yr, 10 k.y., and 10 m.y. time scales. Geology, 29(7), 591-594.

Klock, G.O., Helvey, J.D., 1976. Debris flows following wildfire in north central Washington, Proceedings of the Third Federal Interagency Sedimentation Conference, Denver, Colorado, pp. 91-98.

Lamberti, G.A., Gregory, S.V., Ashkenas, L.R., Wildman, R.C., Moore, K.M.S., 1991. Stream ecosystem recovery following a catastrophic debris flow. Canadian Journal of Fisheries and Aquatic Sciences, 48, 196-208.

Lanini, J.S., Clark, E.A., Lettenmaier, D.P., 2009. Effects of fire-precipitation timing and regime on post-fire sediment delivery in Pacific Northwest forests. Geophysical Research Letters, 36, DOI: 10.1029/2008GL034588.

Larsen, I.J., Pederson, J.L., Schmidt, J.C., 2006. Geologic versus wildfire controls on hillslope processes and debris flow initiation in the Green River canyons of Dinosaur National Monument. Geomorphology, 81, 114-127.

Lavee, H., Kutiel, P., Segev, M., Benyamini, Y., 1995. Effect of surface roughness on runoff and erosion in a Mediterranean ecosystem: the role of fire. Geomorphology, 11, 227-234.

Malamud, B.D., Turcotte, D.L., 1999. Self-organized criticality applied to natural hazards. Natural Hazards, 20, 93-116.

Mangeney, A., 2011. Landslide boost from entrainment. Nature Geoscience, 4, 77-78.

Marchi, L., Arattano, M., Deganutti, A.M., 2002. Ten years of debris-flow monitoring in the Mosacardo Torrent (Italian Alps). Geomorphology, 46, 1-17.

Martin, D.A., Moody, J.A., 2001. Comparison of soil infiltration rates in burned and unburned mountainous watersheds. Hydrological Processes, 15, 2893-2903.

McDonald, G.N., Giraud, R.E., 2002. Fire-related debris flows east of Santaquin and Spring Lake, Utah County, Utah. Utah Geological Survey Technical Report 02-09.

McNeeley, R., Atkinson, D., 1996. Geological Survey of Canada, Radiocarbon dates XXXII. Geological Survey of Canada, Paper 1995-G.

Meyer, G.A., Pierce, J.L., Wood, S.H., Jull, A.J.T., 2001. Fire, storms, and erosional events in the Idaho batholith. Hydrological Processes, 15, 3025-3038.

Meyer, G.A., Wells, S.G., 1997. Fire-related sedimentation events on alluvial fans, Yellowstone National Park, U.S.A. Journal of Sedimentary Research, 67(5), 776-791.

Montgomery, D.R., Abbe, T.B., Buffington, J.M., Peterson, N.P., Schmidt, K.M., Stock, J.D., 1996. Distribution of bedrock and allluvial channels in forested mountain drainage basins. Nature, 381, 587-589.

Moody, J.A., Ebel, B.A., 2012. Hyper-dry conditions provide new insights into the cause of extreme floods after wildfire. Catena, 93, 58-63.

Moon, A.T., Wilson, R.A., Flentje, P.N., 2005. Developing and using landslide frequency models, Proceedings of the International Conference on Landslide Risk Management, Vancouver, BC, pp. 681-690.

Morton, D.M., Campbell, R.H., 1974. Spring mudflows at Wrightwood, southern California. Quarterly Journal of Engineering Geology, 7, 377-384.

Parise, M., Cannon, S.H., 2012. Wildfire impacts on the processes that generate debris flows in burned watersheds. Natural Hazards, 61(1), 217-227.

Parrett, C., Cannon, S.H., Pierce, K.L., 2004. Wildfire-related floods and debris flows in Montana in 2000 and 2001. U.S. Geological Survey, Reston, Virginia Water-Resources Investigations Report 03-4319, 22 pp.
Pierce, J.L., Meyer, G.A., Jull, A.J.T., 2004. Fire-induced erosion and millenial-scale climate change in northern ponderosa pine forests. Nature, 432, 87-90.
Pierson, T.C., Janda, R.J., Thouret, J.C., Borrero, C.A., 1990. Perturbation and melting of snow and ice by the 13 November 1985 eruption of Nevado del Ruiz, Columbia, and consequent mobilization, flow, and deposition of lahars. Journal of Volcanology and Geothermal Research, 41, 17-66.
Plafker, G., Ericksen, G.E., 1978. Nevado Huascaran avalanches, Peru. In: B. Voight (Ed.), Rockslides and avalanches, vol. 1, Natural Phenomena. Elsevier, New York, pp. 277-314.
Prosser, I.P., Williams, L., 1998. The effect of wildfire on runoff and erosion in native *Eucalyptus* forest. Hydrological Processes, 12, 251-265.
Rickenmann, D., Zimmermann, M., 1993. The 1987 debris flows in Switzerland: documentation and analysis. Geomorphology, 8, 175-189.
Rieman, B., Clayton, J., 1997. Wildfire and native fish: issues of forest health and conservation of sensitive species. Fisheries, 22(11), 6-15.
Ritter, D.F., Kochel, R.C., Miller, J.R., 2006. Process geomorphology. Waveland Press, Long Grove, Illinois, 560 pp.
Robichaud, P.R., 2000. Fire effects on infiltration rates after prescribed fire in Northern Rocky Mountain forests, USA. Journal of Hydrology, 231-232, 220-229.
Roering, J.J., Gerber, M., 2005. Fire and the evolution of steep, soil-mantled landscapes. Geology, 33(5), 349-352.
Roghair, C.N., Dolloff, C.A., Underwood, M.K., 2002. Response of a brok trout population and instream habitat to a catastrophic flood and debris flow. Transactions of the American Fisheries Society, 131(4), 718-730.
Santi, P.M., deWolfe, V.G., Higgins, J.D., Cannon, S.H., Gartner, J.E., 2008. Sources of debris flow material in burned areas. Geomorphology, 96, 310-321.
Scott, K.M., 1971. Origin and sedimentology of 1969 Debris flows near Glendora, California. U.S. Geological Survey Professional Paper 750-C, pp. C242-C247.
Sen, P., 1968. Estimates of the regression coefficient based on Kendall's Tau. Journal of the American Statistical Association, 63, 1379-1389.
Sharp, R.P., Nobles, L.H., 1953. Mudflow of 1941 at Wrightwood, southern California. Geological Society of American Bulletin, 64, 547-560.
Slosson, J.E., Havens, G.W., Shuriman, G., Slosson, T.L., 1989. Harrison Canyon debris flows of 1980. Publications of the Inland Geological Society, 2, 235-298.
Spittler, T.E., 1995. Fire and the debris flow potential of winter storms. In: J.E. Keeley, T. Scott (Eds.), Brushfires in California wildlands: ecology and resource management. International Association of Wildland Fire, Fairfield, WA, pp. 113-120.
Stock, J.D., Dietrich, W.E., 2006. Erosion of steepland valleys by debris flows. Geological Society of America Bulletin, 118(9/10), 1125-1148.
Stoffel, M., 2010. Magnitude-frequency relationships of debris flows -- A case study based on field surveys and tree-ring records. Geomorphology, 116, 67-76.
Swanson, F.J., 1981. Fire and geomorphic processes. USDA Forest Service, General Technical Report WO-26 401-420.

Swanston, D.N., 1991. Natural processes. In: W.R. Meehan (Ed.), Influences of forest and rangeland management on salmonid fishes and their habitats. American Fisheries Society Special Publication 19, Bethesda, MD.
Theobald, D.M., Romme, W.H., 2007. Expansion of the US wildland-urban interface. Landscape and Urban Planning, 83(4), 340-354.
Thompson, M.P., Calkin, D.E., Finney, M.A., Ager, A.A., Gilbertson-Day, J.W., 2011. Integrated national-scale assessment of wildfire risk to human and ecological values. Stochastic Environmental Research and Risk Assessment, 25(6), 761-780.
Thurber Engineering, Golder Associates, 1993. The Cheekye River terrain hazard and land-use study, final report. Report prepared for British Columbia Ministry of Environment, Lands and Parks Burnaby, B.C.
Vallance, J.W., Scott, K.M., 1997. The Osceola mudflow from Mount Rainier: sedimentology and hazad implications of a huge clay-rich debris flow. Geological Society of America Bulletin, 109(2), 143-163.
van Steijn, H., 1996. Debris-flow magnitude-frequency relationships for mountainous regions of Central and Northwest Europe. Geomorphology, 15, 259-273.
van Steijn, H., 1999. Frequency of hillslope debris flows in the Bachelard Valley (French Alps). In: M. Panizza, M. Soldati, M. Bertacchini, T.W.J. Van Asch, S. Malmusi (Eds.), The Erasmus 96-97 Programme in Geomorphology: Intensive Course in the French Alps and Students' Mobility. Dipartimento di Scienze della Terra, Universita degli Studi di Modena e Reggio Emilia, pp. 15-24.
Wells, W.G., 1987. The effects of fire on the generation of debris flows in southern California. In: J.E. Costa, G.F. Wieczorek (Eds.), Geological Society of America Review of Engineering Geology, pp. 105-114.
Wieczorek, G.F., Harp, E.L., Mark, R.K., Bhattacharyya, A.K., 1988. Debris flows and other landslides in San Mateo, Santa Cruz, Contra Costa, Alameda, Napa, Solano, Sonoma, Lake, and Yolo counties, and factors influencing debris-flow distribution. In: S.D. Ellen, G.F. Wieczorek (Eds.), Landslides, Floods, and Marine Effects of the Storm of January 3-5, 1982, in the San Francisco Bay Region, California, U.S. Geological Survey Professional Paper 1434, pp. 133-162.
Wilkerson, F.D., Schmid, G.L., 2003. Debris flows in Glacier National Park, Montana: geomorphology and hazards. Geomorphology, 55(2003), 317-328.
Wondzell, S.M., King, J.G., 2003. Postfire erosional processes in the Pacific Northwest and Rocky Mountain regions. Forest Ecology and Management, 178, 75-87.
Woods, S.W., Balfour, V.N., 2010. The effects of soil texture and ash thickness on the post-fire hydrological response from ash-covered soils. Journal of Hydrology, 393(3-4), 274-286.
Woods, S.W., Birkas, A., Ahl, R., 2007. Spatial variability of soil hydrophobicity after wildfires in Montana and Colorado. Geomorphology, 86, 465-479.

Figure 1. Field sites for debris flow fan dimensions collected for this study. Mountain ranges where debris flows were mapped during this study are shown in gray, with the total number of debris flows occurring in that mountain range noted. Clusters of debris flows occurred in some watersheds, and these are titled in black, with the number of debris flows in that watershed given. Note that the number of debris flows occurring in a watershed is also included in the total amount for the corresponding mountain range; for example, all debris flows mapped in the Bitterroot Mountains (*n*=18) occurred in Laird Creek (*n*=18). Clusters of debris flows were likely produced by the conjunction of a recent high severity burn and intense localized rainfall. Relevant fire perimeters are shown in orange.

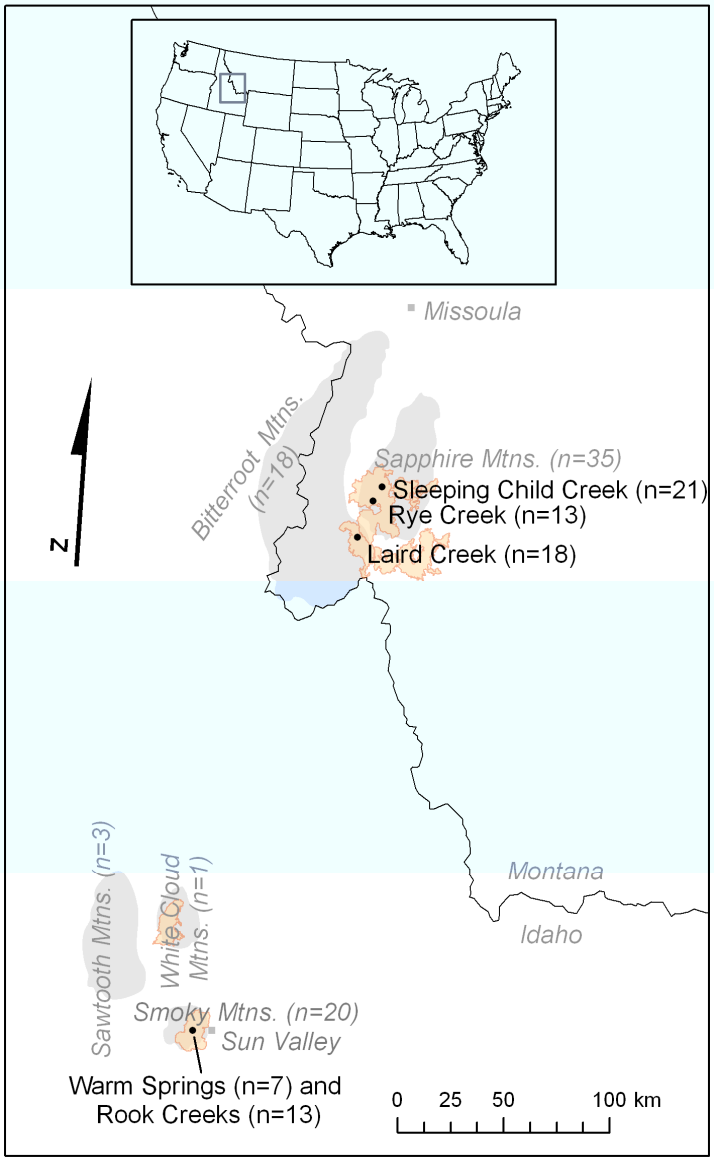

Figure 2. The abrupt transition from rill to gully head is physical evidence for runoff initiation. Note abrupt downcutting on the order of 0.8 m. Gully head is finger-shaped. Scarp indicating landsliding is absent.

Figure 3. Post-fire debris flow in the Fourth of July Creek drainage in the White Cloud Mountains. Note the rejuvenated gully in the background, and the levees at lower left and middle right.

Figure 4. Detail of fan deposit in Rye Creek in the Sapphire Mountains of Montana, representing a typical deposit for the region. Note size distribution of clasts, from cobble to sand.

Figure 5. This photograph shows topography typical of the Sapphire and southern Bitterroot Mountains, where a cluster of debris flows occurred following the extensive fires of 2000. Three paleofan perimeters are roughly outlined in yellow. One of the recent debris flows entered the backyard of the house shown in this photo, which is built atop a much larger paleofan. A second fan is visible at right. From the vantage of this photo, taken from atop a third debris flow fan, it is evident that alternating debris flow fan/paleofan deposits define the topography of the valley floor as well as the course of Laird Creek (stream course shown in blue). Debris flow events occurred following the fires of 2000 atop each of these three paleofans, but fan boundaries were already obscured by regrowth of vegetation by the time this photo was taken in 2008.

Figure 6. Geographical distribution of debris flows in catalog, by nation.

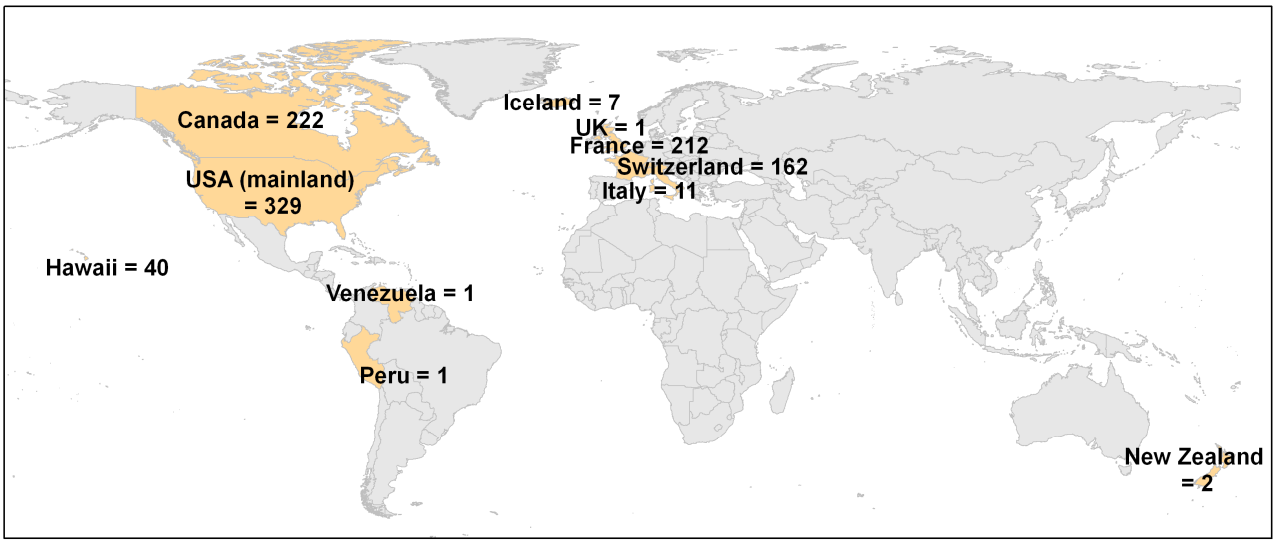

Figure 7. Debris flow volumes, grouped by location. Only locations with more than five debris flows are shown in this figure. Specific locations were known for some debris flows (e.g. Sleeping Child Creek), while only general locations were known for others (e.g. Switzerland). The highest degree of specificity was retained in this graph, resulting in some groupings being broader geographically than others. Post-fire debris flows are plotted in red. Location codes identify these debris flows in the catalog.

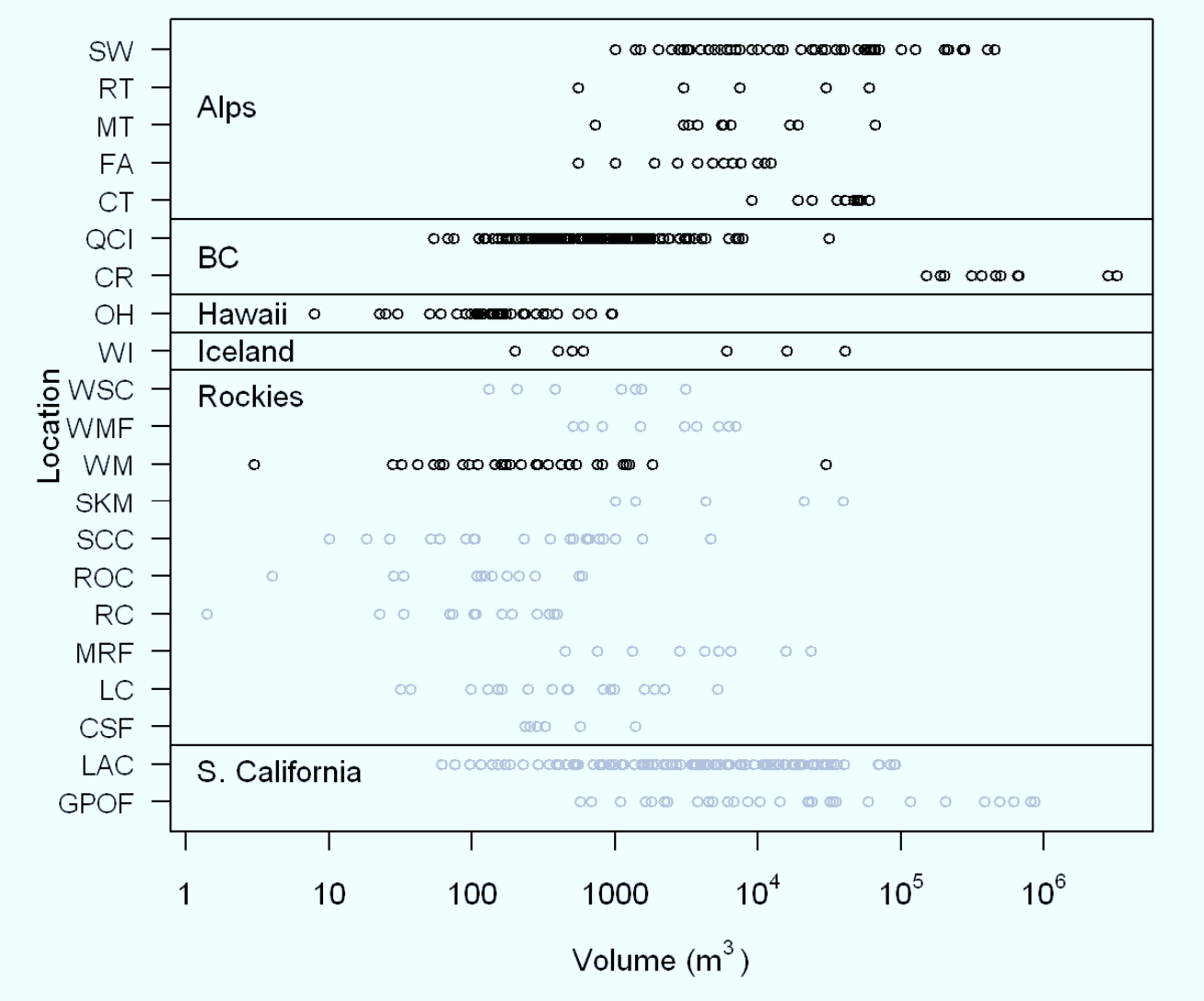

Figure 8. Boxplots of volumes of post-fire and non-fire-related debris flows.

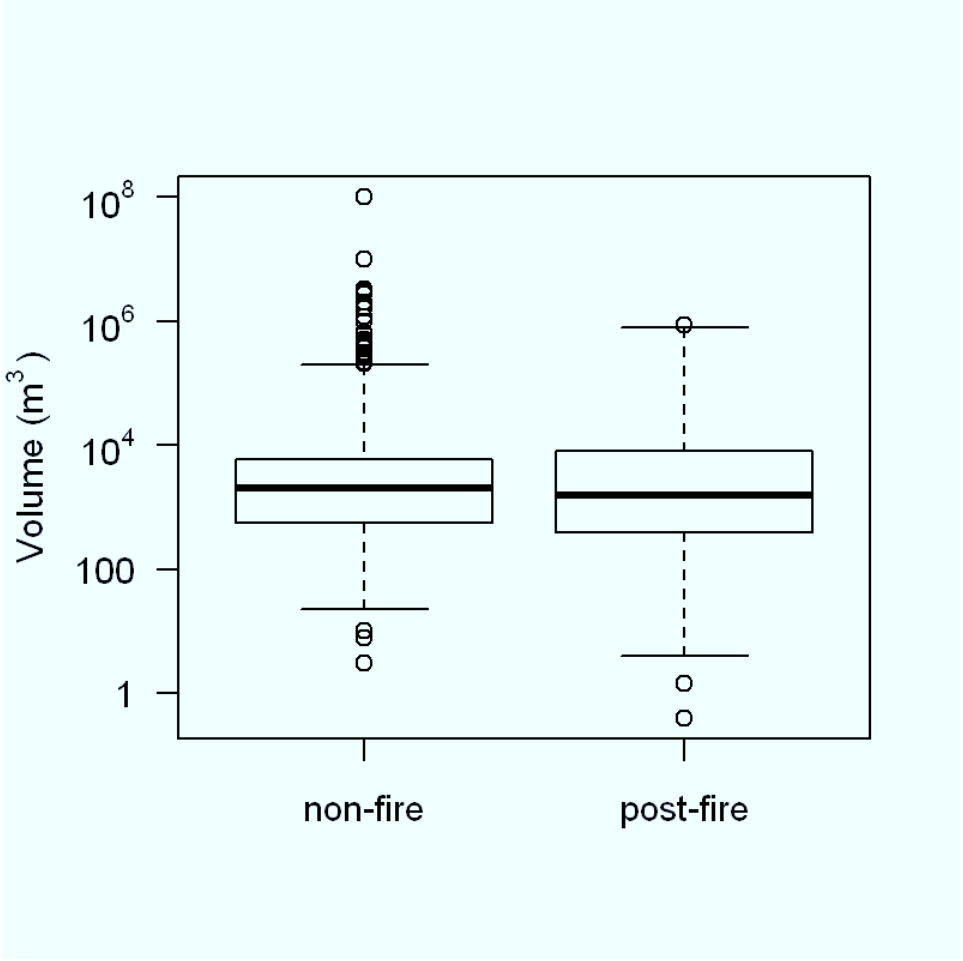

Figure 9. Frequency-magnitude distribution of post-fire and non-fire-related debris flows.

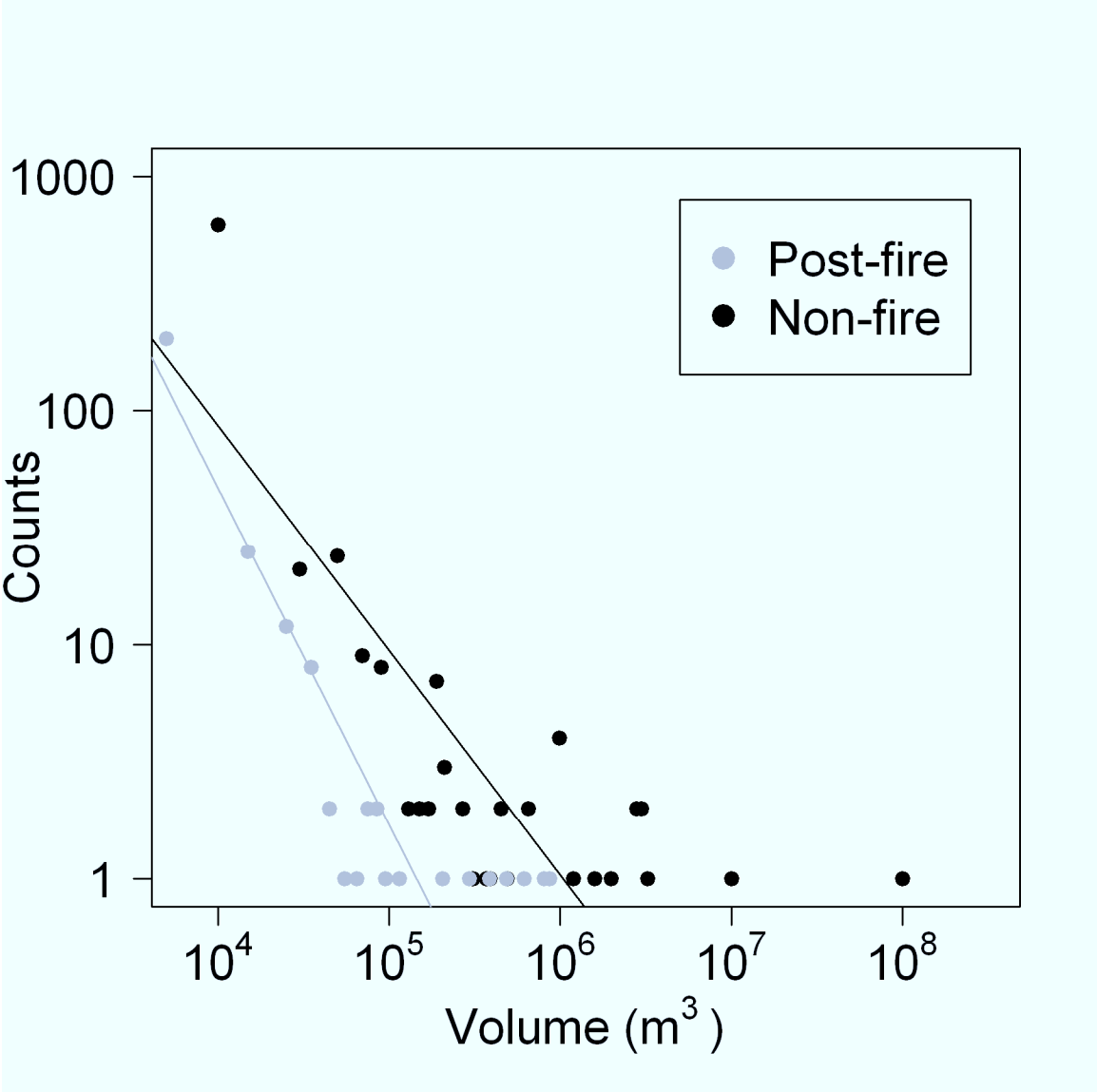

Figure 10. 95% confidence interval of slope parameters of the frequency-magnitude distribution for post-fire and non-fire-related debris flows.

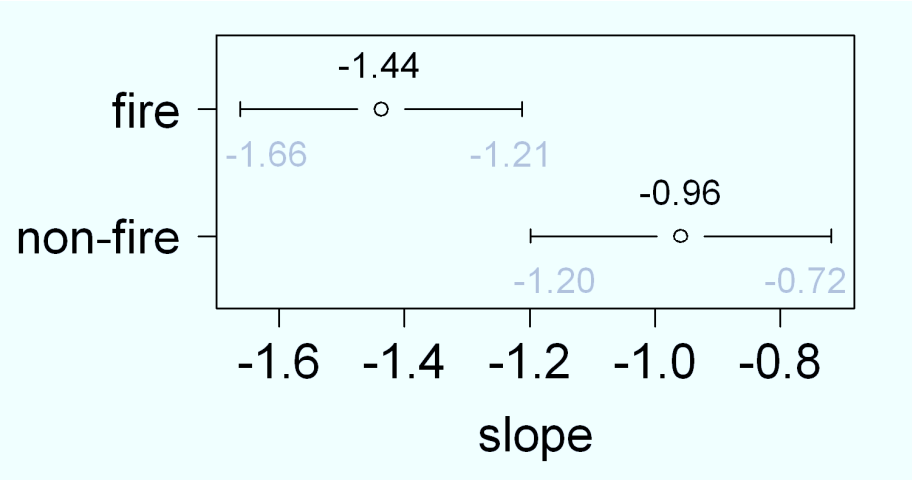

Figure 11. Empirical cumulative distribution functions (ECDFs) of post-fire and non-fire-related debris flow volumes

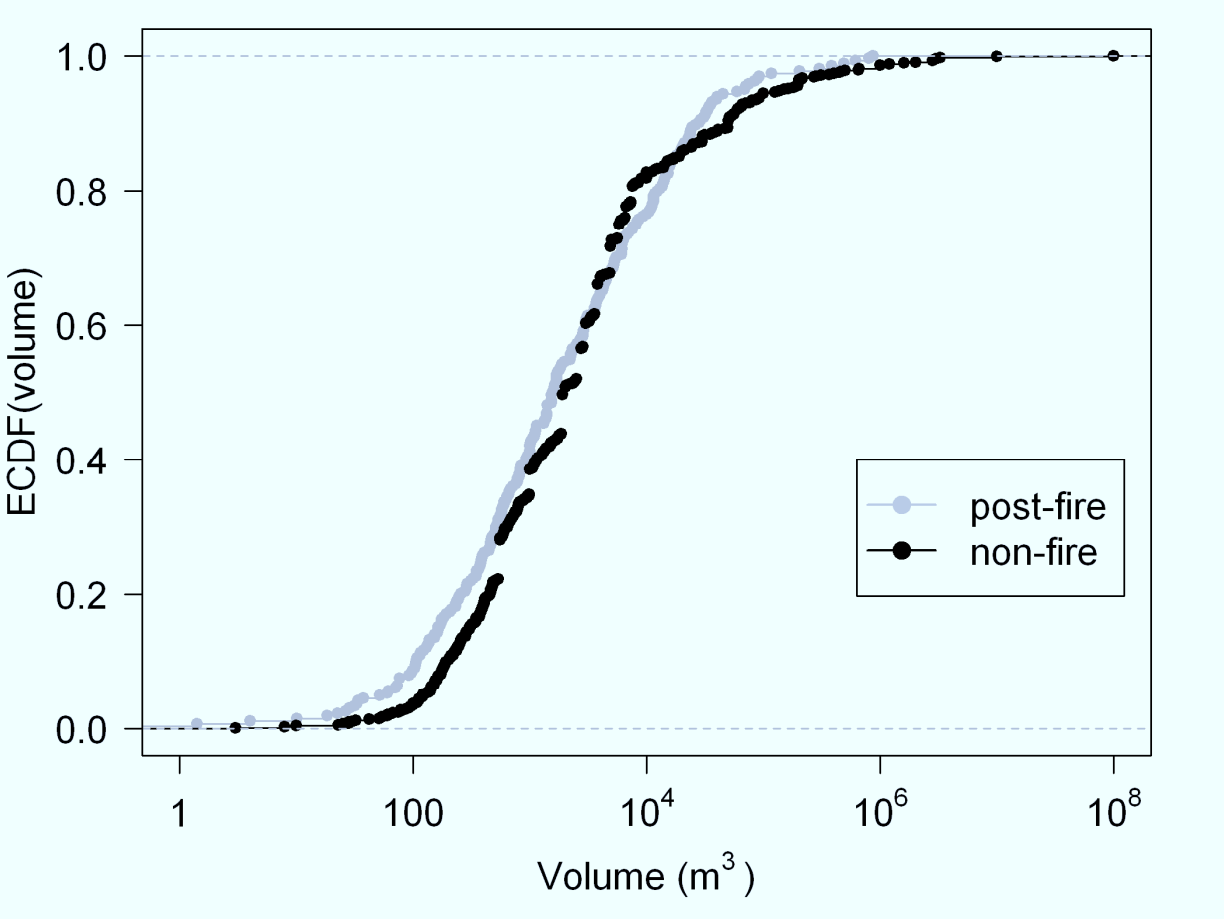

Figure 12. Boxplots comparing the volume of debris flows initiating through landslides ("L", *n* = 104) to those initiating through runoff ("RO", *n* = 383).

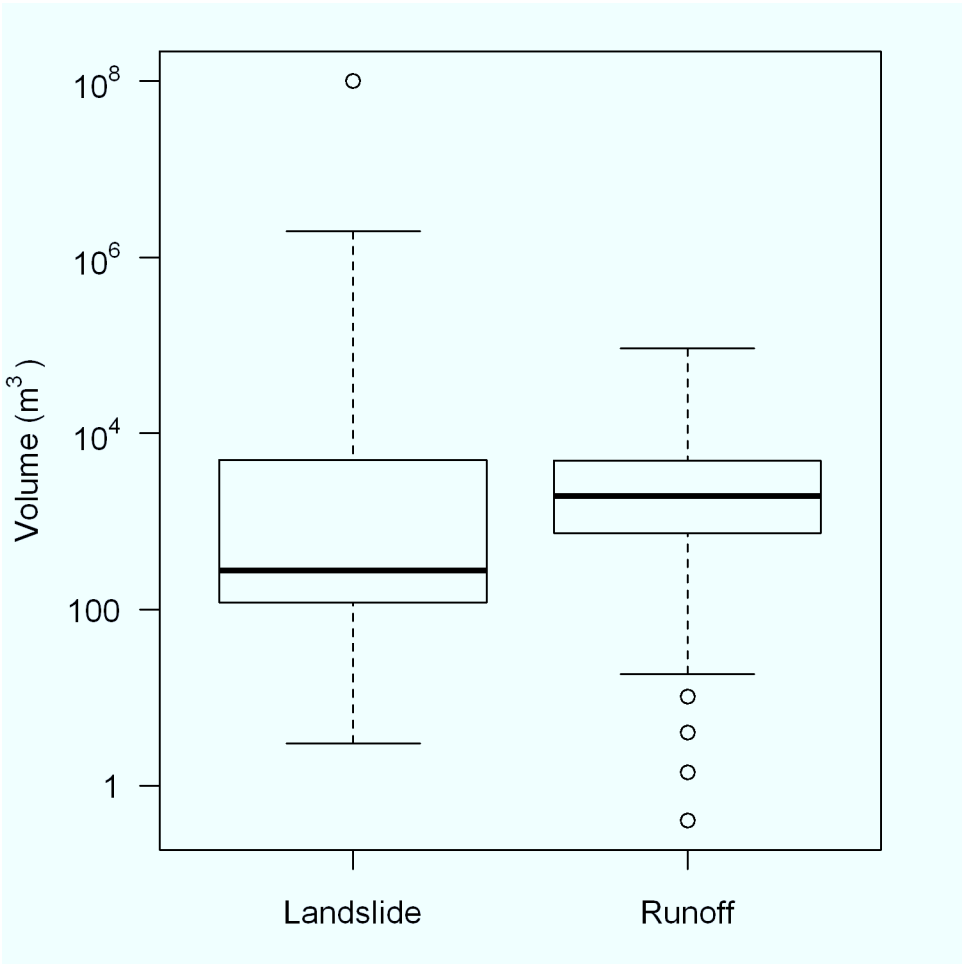

Figure 13. Boxplots comparing runoff-initiated debris flow volumes, for non-fire-related (*n* = 199) and post-fire events (*n* = 184).

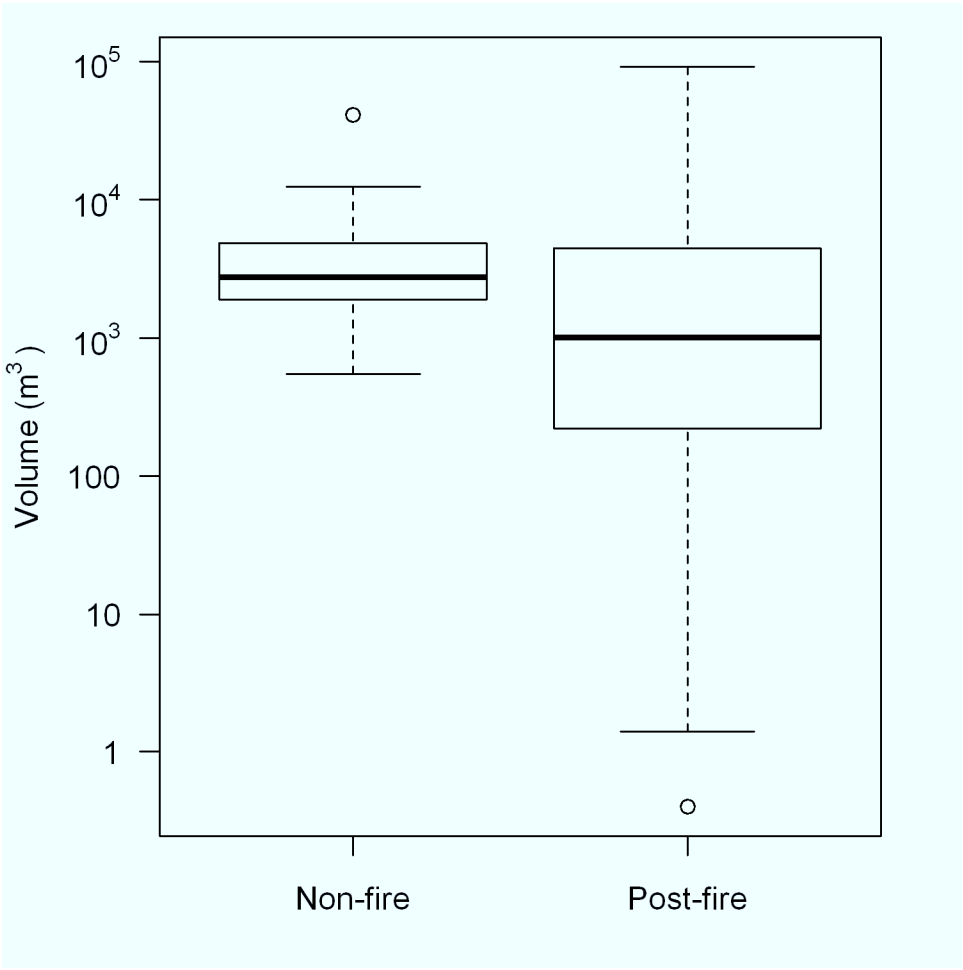

Table 1. Sites where debris flow data were collected in the field for this study. Likely dates of debris flows were based on: 1) US Geological Survey precipitation stations, as reported by Parrett et al (2004), or 2) local newspaper reports (Wutz et al 2010), as indicated by superscripts. Peak 5-minute precipitation intensity and recurrence interval were derived from precipitation data in Parrett et al (2004). Three-hour total precipitation was recorded by nearby NEXRAD stations. Initiation mechanism was based on field observations during this study.

Site	Location	State	Number of debris flow events	Associated fire event	Likely event dates	Peak 5-minute precipitation intensity (cm/h)	3-hour total precipitation (mm)	Precipitation recurrence interval (years)	Initiation mechanism
Frenchman Creek	Sawtooth Mountains	Idaho	1	NA					firehose effect
Smiley Creek	Sawtooth Mountains	Idaho	2	NA					unknown
Rooks Creek	Smoky Mountains	Idaho	13	Castle Rock Fire, 2007	June 2009, multiple days [2]	No data	1.2 – 5.1		runoff
Warm Springs Creek	Smoky Mountains	Idaho	7	Castle Rock Fire, 2007	June 2009, multiple days [2]	No data	2.5 – 12.7		runoff
Fourth of July Creek	White Cloud Mountains	Idaho	1	unknown					runoff

Laird Creek	Bitterroot Mountains	Montana	18	Bitterroot Fires, 2000	15, 20, 21 July 2001 [1]	2.7 – 6.4	5.1 – 31.8	<2 - 25	runoff
Sleeping Child Creek	Sapphire Mountains	Montana	21	Bitterroot Fires, 2000	30 Sept. – 1 Oct., 2000; 15 and 21 July 2001 [1]	5.8 - 6.4	12.7 – 19.1	5	runoff
Two Bear Creek	Sapphire Mountains	Montana	1	Bitterroot Fires, 2000	30 Sept. – 1 Oct., 2000; 15 and 12 July 2001 [1]	5.8 – 6.4	12.7 – 19.1	5	runoff
Rye Creek	Sapphire Mountains	Montana	13	Bitterroot Fires, 2000	30 Sept. – 1 Oct., 2000; 15 and 20 July 2001 [1]	6.7		10	runoff

Table 2. Location name, code, description, source literature, number of debris flows, and whether debris flows were post-fire, for locations in Figure 7. Debris flow data collected for this study are shown in italics.

Location name	Location Code	Location description	Source	n	post-fire?
Chalance Torrent	CT	Chalance Torrent, French Alps	Helsen, Koop, and van Steijn (2002)	14	no
Cheekye River	CR	British Columbia, Canada	cited in Jakob and Friele (2010)	13	no
Coal Seam Fire	CSF	near Glenwood Springs, Colorado, USA	Gartner (2005)	6	yes
French Alps	FA	French Alps	van Steijn (1999)	198	No
Grand Prix/Old Fire	GPOF	southern California, USA	Gartner (2005)	27	yes
Laird Creek	*LC*	*Bitterroot Mountains, Northern Rocky Mountains, Montana, USA*		*18*	*yes*
Los Angeles County	LAC	Los Angeles County, California, USA	Scott (1971), as cited in Gartner, Bigio, and Cannon (2004); Sue Cannon, personal communication	102	yes
Missionary Ridge Fire	MRF	near Durango, Colorado, USA	Gartner (2005)	8	yes
Moscardo Torrent	MT	Italian Alps	Marchi et al (2002)	10	no
Oahu	OH	Oahu, Hawaii, USA	Sue Cannon, personal communication	40	no
Queen Charlotte Island	QCI	British Columbia, Canada	Oldrich Hungr, personal communication; see also Hungr et al. (2008)	174	no
Ritigraben Torrent	RT	Swiss Alps	Stoffel (2010)	62	no
Rooks Creek	*ROC*	*Smoky Mountains, near Ketchum, Idaho, USA*		*13*	*yes*
Rye Creek	*RC*	*Sapphire Mountains, Northern Rocky Mountains,*		*13*	*yes*

		Montana, USA			
Sleeping Child Creek	*SCC*	*Sapphire Mountains, Northern Rocky Mountains, Montana, USA*		*21*	*yes*
Storm King Mountain	SKM	near Glenwood Springs, Rocky Mountains, Colorado, USA	Cannon, Powers, Savage (1998)	7	yes
Switzerland	SW	Switzerland	Dieter Rickenmann, personal communication; see also Rickenmann and Zimmermann (1993)	99	no
Warm Spring Creek	*WSC*	*Smoky Mountains, near Ketchum, Idaho, USA*		*7*	*yes*
Wasatch Front	WM	Wasatch Front and Plateau, Utah, USA	Cannon (1989)	30	no
Wasatch Front	WMF	Wasatch Front and Plateau, Utah, USA	Gartner (2005); McDonald and Giraud (2002); Santi et al (2008)	9	yes
Westfjords, Iceland	WI	Westfjords, Iceland	Conway et al (2010)	7	no

Table 3. Selected statistics for post-fire and non-fire-related debris flow volumes. Volumes are in m^3.

	Minimum volume	Median volume	Maximum volume	Slope of frequency-magnitude distribution	n
Post-fire	0.4	1,579	864,308	-1.44	264
Non-fire-related	3	2,000	100,000,000	-0.96	724

Chapter 3.

The relationship of large fire occurrence with drought and fire danger indices in the western USA, 1984-2008: the role of temporal scale

Karin L. Riley[AB], John T. Abatzoglou[C], Isaac C. Grenfell[D], Anna E. Klene[E], and Faith Ann Heinsch[D]

[A] University of Montana, Department of Geosciences, Missoula, MT 59812

[B] Corresponding Author. Telephone: +1 406 329 4806; fax: +1 406 329 4877; email: kriley@fs.fed.us

[C] University of Idaho, Department of Geography, Moscow, ID 83844

[D] USDA Forest Service, Rocky Mountain Research Station, Fire Sciences Laboratory, 5775 W US Highway 10, Missoula, MT 59808

[E] University of Montana, Department of Geography, Missoula, MT 59812

Abstract

The relationship between large fire occurrence and drought has important implications for fire hazard prediction under current and future climate conditions. The primary objective of this study was to evaluate correlations between drought and fire-danger-rating indices representing short- and long-term drought, to determine which had the strongest relationships with large fire occurrence at the scale of the western United States during the years 1984-2008. We combined 4-8 km gridded drought and fire-danger-rating indices with information on fires greater than 1000 acres from the Monitoring Trends in Burn Severity project. Drought and fire danger indices analyzed were: monthly precipitation (PPT), Energy Release Component for fuel model G (ERC(G)), Palmer Drought Severity Index (PDSI), 3-month Standardized Precipitation Index (SPI3), SPI6 , SPI9, SPI12, and SPI24. To account for differences in indices across climate and vegetation assemblages, indices were converted to percentile conditions for each pixel, to indicate the relative anomaly in conditions during large fires. Across the western US,

correlations between area burned and short-term indices ERC(G) and PPT percentile were strong (R^2 = 0.92 and 0.89 respectively), as were correlations between number of fires and these indices (R^2=0.94 and 0.93 respectively). As the period of time tabulated by the index lengthened, correlations between fire occurrence and indices weakened: PDSI and 24-month SPI percentile showed weak or negligible correlations with area burned (R^2 = 0.25 and -0.01 respectively) and number of large fires (R^2 = 0.3 and 0.01 respectively). This result suggests the utility of shorter-term rather than longer-term indices in fire danger applications. We attribute strong correlations between shorter-term indices and fire occurrence to strong associations between these indices and moisture content of dead fuels, which are the primary carriers of surface fire.

Brief summary for table of contents

Shorter-term drought and fire-danger-rating indices, in particular Energy Release Component and monthly precipitation totals, were strongly correlated with area burned and number of large fires in the western US during the period 1984-2008, likely due to strong associations of these indices with dead fuel moistures. Longer-term indices (Palmer Drought Severity Index and SPI24) showed weak or negligible correlations with area burned and number of large fires.

Additional keywords: precipitation, ERC, PDSI, SPI, area burned, number of fires, MTBS, fire danger

Introduction

Estimation of burn probability and wildland fire risk to highly valued resources influences land management planning, budgeting for firefighting and fuels reduction work, and positioning of suppression resources in the United States (Ager et al., 2010; Calkin et al., 2011; Finney et al., 2011b). Current modeling efforts have produced burn probability maps for the continental US which are statistically similar to recent fire activity (Finney et al., 2011b), and statistical models that incorporate climate data have exhibited better-than-random prediction of area burned (Westerling et al., 2002; Preisler and Westerling, 2007; Preisler et al., 2009), but a

number of challenges in fire prediction remain. Large fires occur stochastically, in response to lightning produced by localized convective storms and human ignitions, making prediction of the location and timing of fires difficult. As the climate changes, temperature and precipitation regimes fluctuate, which may affect the occurrence of large fires. Given these uncertainties, it is important to understand the mechanisms by which various drought and fire danger indices (which capture different timescales of drought) are empirically related to large fire occurrence, and the strength of these relationships.

Another challenge in studies of wildland fire and climate is that large fires are rare events. Accordingly, much previous work on fire and climate has taken place at large spatial scales at annual timesteps, in order to encompass a large enough sample size of fires for statistical analysis to be possible. In the case of fire history work, most studies take place at a regional scale and at an annual timestep which chronicles both drought (inferred from tree ring width) and fire occurrence (based on positioning of fire scars relative to tree rings) (e.g. Baisan and Swetnam, 1990; Swetnam and Betancourt, 1998; Hessl et al., 2004; Heyerdahl et al., 2008b; Morgan et al., 2008). Some studies have linked some of the variability in fire occurrence and area burned with synoptic weather patterns such as persistent high pressure blocking ridges and coupled atmosphere-ocean teleconnections (e.g. El Niño-Southern Oscillation and Pacific Decadal Oscillation) that correlate with droughts (e.g. Trouet et al., 2009; Abatzoglou and Kolden, 2011). ENSO and PDO fluctuate on annual timesteps, and thus many of these studies focus at this timescale. However, daily and monthly fluctuations in weather are strong determinants of fire ignition and spread. Recently, finer-scale weather data and a comprehensive database of large fires have become available, enabling analysis of the relationship between drought and fire at a more detailed spatial and temporal scale. An improved understanding of the time-scales and means through which climate and weather influence fire occurrence would be beneficial to fire prediction efforts as well as operational fire management, and provide a way for researchers to link predictions of climate change with their potential effect on future fire occurrence.

Precipitation is related to fire occurrence via several mechanisms. 1) In dead fuels such as litter and downed woody debris, fuel moisture is controlled by environmental conditions including precipitation, relative humidity, solar radiation, and temperature. In the absence of precipitation, dead vegetation (fuels) will dry out, converging toward ambient relative humidity

over a period of days or weeks, the period increasing with fuel diameter (Fosberg, 1971). 2) During prolonged dry periods (which occur seasonally in some areas), live herbaceous and woody shrub vegetation may enter dormancy or die, contributing to the loading of fine dead surface fuels (<0.25" diameter), which are the primary carriers of surface fire (Scott and Burgan, 2005). 3) Live fuels decrease in moisture content during dry periods, and the proportion of flammable compounds may increase (Matt Jolly, personal communication). 4) Ignition and propagation of fire is more likely when fuels are dry, and fire rates of spread are higher (Rothermel, 1972; Andrews et al., 2003; Scott and Burgan, 2005).

Live and dead fuel moistures thus fluctuate across a range of timescales, from daily (due to rain events), to seasonally (in the western US, new live vegetation typically grows during spring and matures and/or cures during dry summers), to decadally (in response to extended droughts). Various fire danger and drought metrics utilize different temporal scales, which are implicitly related to these fuel moisture dynamics, but more work is needed to relate these metrics to fire occurrence in the western US, both empirically and physically. Use of indices based on fuel moisture values derived from recent weather could strengthen fire modeling efforts, since some frequently used metrics may not be directly related to fire ignition and behavior.

We quantified the correlation of eight drought and fire danger metrics with large (>1000 acres) fire occurrence, defined using two criteria: area burned and number of fires. The drought and fire danger indices included in this study were: Standardized Precipitation Index (SPI) calculated for 3, 6, 9, 12, and 24 month intervals, Palmer Drought Severity Index (PDSI), monthly precipitation totals (PPT), and Energy Release Component (ERC). These indices were selected based on their common usage in the literature regarding drought and fire in the western US, and/or our assessment of their potential for capturing the relationship between drought and fire occurrence. The goals of this study were to: 1) examine which, if any, of these metrics were strongly related to fire occurrence across the western US, independent of ecoregion, climatic zone, and vegetation type, and 2) investigate whether the timescale of the indices affected the strength of their correlations with fire occurrence. A metric that is strongly correlated with fire occurrence across this region could be utilized with high confidence in fire prediction work. Examining which metrics are strongly correlated with fire occurrence suggests physical mechanisms linking drought and fire.

Methods

Study area

The western US was chosen for this study because it spans a number of diverse fire-adapted ecoregions. In order to delineate the study area (Figure 1) from the grasslands of the Great Plains, we used Omernik ecoregions (Omernik, 1987).

Data sources: addressing challenges in reporting

Fire records

Fire records were obtained from the Monitoring Trends in Burn Severity (MTBS) project, conducted jointly by the US Forest Service and US Geological Survey, which maps the extent of large fires since 1984 based on Landsat imagery (Eidenshink et al., 2007). Fires included in our study (n = 5976) were limited to those that had centroids within our study area boundary, occurred between 1 January 1984 and 31 December 2008, and were larger than 404.7 ha (1000 acres), since large fires burn the vast majority of the area in this region (Strauss et al., 1989). We used data on fire perimeters, areas, locations, and discovery dates provided by MTBS.

The MTBS dataset addresses some issues that previously existed in fire records due to inconsistent and incomplete reporting of wildland fires (Brown et al., 2002; Schmidt et al., 2002).. No single comprehensive database tracks all fires in the US, so a complete record of fires must be compiled from records of multiple federal agencies (US Department of Agriculture Forest Service uses one system, a second system is employed by the US Department of Interior (USDOI) Fish and Wildlife Service, and a third system is used by USDOI's Bureau of Land Management, Bureau of Indian Affairs, and National Park Service) as well as non-federal records (state databases, National Association of State Foresters records, and the US Fire Administration's national Fire Incident Reporting System). Compiled records are subject to several issues, including incongruent reporting standards. For example, more than half of non-federal fire records lack information on date, location, or size, meaning that they cannot be used for analyses with spatial or temporal questions (Karen Short, personal communication). The MTBS project has determined the spatial locations and discovery dates of all fires in its dataset through geolocated burn scars, an advantage of this dataset. A second issue in compilations is

duplicate records, which can cause overestimates of area burned on the order of 40% (Karen Short, personal communication). Duplicate records occur most frequently where large fires cross land ownership boundaries, causing records to appear in multiple land agency reporting systems. Since the MTBS dataset is based on changes in spectral signatures in Landsat imagery, duplicate records are eliminated and some previously unreported fires are detected. Compilations of fire records may also suffer from omissions, especially of smaller fires, which can cause underestimates of fire numbers. Because the MTBS dataset includes only fires larger than 404.7 ha (1000 acres) in the western United States, this problem is minimized, but analysis is confined to large fire events.

The intention of MTBS is to track wildland fires, but some prescribed fires have been included in the database through detection of changes in spectral signatures. At the time of this study, MTBS did not state whether each fire was prescribed or wildland, so we were unable to separate them. Data on daily fire progression is lacking or not readily available from MTBS or other sources, meaning the contribution of daily winds (an important factor in fire growth) could not be quantified for this study.

Drought and fire danger indices

The eight drought and fire danger indices analyzed in this study provide a means for assessing relative wetness or dryness of the fire environment, and may serve as predictors of water availability, vegetation health, and fire danger. We utilized spatially and temporally complete high-resolution gridded climate and meteorological datasets (Figure 2). Monthly climate data from Parameter-elevation Regressions on Independent Slopes Model (PRISM; Daly et al., 1994a) at 4-km horizontal resolution were used to derive the PPT, PDSI and SPI indices following Kangas and Brown (2007). The drought indices were calibrated to the 1895-2009 period of record, making them more robust than monthly drought indices calculated over shorter time periods. A complementary dataset developed by Abatzoglou (2011) provided a spatially and temporally complete daily meteorological dataset from 1979-2010 upsampled to 8-km resolution by employing high-frequency meteorological conditions from the North American Land Data Assimilation System (NLDAS) that is then bias-corrected using PRISM. The resultant dataset provided daily maximum and minimum temperatures, relative humidity, daily precipitation amount and duration, temperature, and state-of-the-weather code for 1300 local

time, all components necessary for NFDRS calculations of ERC(G). This study utilized the products of these efforts: PPT, PDSI, SPI3, 6, 9, 12, and 24 at a 4-km scale and monthly timestep, and ERC(G) at an 8-km scale on a daily timestep.

Previous work on fire and climate faced challenges in obtaining weather records; these gridded datasets address some of these challenges. For example, Remote Automated Weather Stations (RAWS) used for fire danger calculations are often switched off when fire season ends, meaning that weather records are temporally incomplete. Until recently, weather data has typically been available only at sparse point locations with weather stations or summarized at coarse resolution. Researchers were presented with the choice of using weather data from a single station as a proxy for a large area, or using a dataset such as the National Climatic Data Center climate division data, which averages conditions from weather stations over large areas that do not necessarily correspond to ecoregion boundaries (e.g. Balling et al., 1992; Littell et al., 2009). Microclimates can vary widely within a few square kilometers, especially in the mountainous terrain that characterizes much of the western US (Thornthwaite, 1953; Sellers, 1965; Holden et al., 2011), suggesting that coarse-resolution climate division data may not be representative of conditions at remote wildfire locations, as was noted by Westerling *et al.* (2002).

By applying physically- and statistically-based algorithms to weather station records, recent efforts have produced gridded weather datasets with a resolution of several kilometers, such as the ones used in this study (Daly et al., 1994b; Abatzoglou, 2011; Thornton et al., 2012). Such datasets have made more detailed analysis possible by avoiding the spatial limitations of climate division datasets and the often temporally sporadic and spatially non-uniform data from weather stations. Gridded datasets at 4-8 km resolution cannot account for all microclimate variability, but represent an advance in this effort.

Below, we briefly describe the calculation of each index and previous work relating this index to fire occurrence. Throughout this manuscript, we qualitatively define the strength of correlations as follows: weak ($R^2 < 0.45$), moderate ($0.45 < R^2 < 0.8$), or strong ($0.8 <= R^2 <= 1$).

Palmer Drought Severity Index (PDSI)

Palmer (1965) outlined calculation of his drought metric as "a first step toward understanding drought," but the metric has since become widely institutionalized, especially for estimating agricultural drought. Positive values of PDSI suggest wetter-than-normal conditions, and negative values suggest drought (-1 = mild drought, -2 = moderate drought, -3 = severe drought, and -4 = extreme drought) (Palmer, 1965). The PDSI uses a water balance method which adds precipitation to soil moisture in the top two layers of soil, while a simple temperature-driven evapotranspiration algorithm (Thornthwaite, 1948) removes it. The calculation of PDSI is autoregressive, based on a portion of the current month's value and the preceding value (Guttman, 1998). Thus, PDSI has no inherent time scale, with PDSI values having different "memories" varying from 2 to more than 9 months depending on the location (Guttman, 1998). The spatial scale of PDSI also varies, since the index can be calculated for a single weather station or a number of stations may be averaged, as in the case of climate division data.

Criticisms of the PDSI are numerous. The algorithm lacks information on important drivers of evapotranspiration, vegetation curing, and dead fuel moisture, including relative humidity, solar radiation, and wind speed (Sheffield et al., 2012). All precipitation is assumed to be rain, meaning the algorithm is potentially ill-suited for areas where a significant proportion of the precipitation is snowfall. Hence, PDSI has been found to be only weakly to moderately correlated with soil moisture ($r = 0.5\text{-}0.7$, equivalent to $R^2 = 0.25 – 0.49$), with the strongest correlation in late summer and autumn, corresponding with fire season in much of the western US (Dai et al., 2004). Due to data and processing limitations, Palmer developed the index for nine climate divisions in the Midwest, resulting in empirically derived constants that are not locally calibrated for other locations (Palmer, 1965). Consequently, the PDSI's value has been found to vary across precipitation regimes, with a single value having different meanings in different areas (Guttman et al., 1992; Guttman, 1998). In addition, PDSI values are sensitive to the time period used to calibrate the metric (Karl, 1986).

Despite these shortcomings and lack of a clear mechanism relating PDSI to fire occurrence, the PDSI is the index most commonly used to assess drought in the fire literature (Table 1; Baisan and Swetnam, 1990; Swetnam and Betancourt, 1998; Hessl et al., 2004; Heyerdahl et al., 2008b). For fire history studies, PDSI is often the only available metric.

Current-season PDSI values have also been related to contemporary fire occurrence in some ecosystems of the western US, although correlations are rarely strong (Table 1).

Monthly precipitation totals (PPT)

Several studies have used measured precipitation amount to relate drought to fire occurrence. This metric is simple to measure and calculate; however, because precipitation regimes vary across climatic regions, amounts must be normalized to local records in order to indicate departure from normal conditions. Littell *et al.* (2009) found seasonal precipitation to be a significant factor in multivariate models predicting area burned for some but not all ecoregions in the western US, with negative summer precipitation included in models for 7 of 16 ecoregions. Balling *et al.* (1992) found total annual precipitation had a Spearman's rank correlation of -0.52 to -0.54 with area burned in Yellowstone National Park, a stronger correlation than they found with PDSI (Table 1).

Standardized Precipitation Index (SPI)

The SPI is calculated as "the difference of precipitation from the mean for a specified time period divided by the standard deviation" (McKee et al., 1993); where precipitation amounts are not normally distributed, they must be first converted to a normal distribution (Lloyd-Hughes and Saunders, 2002). Benefits of the SPI include: 1) it can be used to derive probability of precipitation deviation, 2) it is normalized, so wet and dry climates are represented in similar fashions (McKee et al., 1993), 3) SPI spectra exhibit similar patterns at all locations, meaning the values are comparable across regions (Guttman, 1998), and 4) the index can be calculated for any time length in order to capture short- or long-term drought. Despite the advantages of the SPI, we found only one study relating SPI to fire occurrence: Fernandes *et al.* (2005) found strong correlations between summer 3-month SPI (SPI3) and anomalies in fire incidence in the Western Amazon.

Energy Release Component (ERC)

The Energy Release Component (ERC), an index in the US National Fire Danger Rating System (NFDRS), provides an approximation of dryness based on estimates of fuel moisture (Andrews et al., 2003). ERC is a continuous variable calculated from a suite of meteorological and site variables, including relative humidity, temperature, precipitation duration, weather station latitude, and day of year (Cohen and Deeming, 1985). ERC is calculated daily and is thus more dynamic than current implementations of PDSI and SPI, since it is sensitive to daily relative humidity and precipitation timing and duration (i.e., large rain events cause a significant reduction in ERC). ERC calculation is also affected by fuel loadings in different size classes. For example, in this study, ERC was calculated for fuel model G, which includes a substantial loading of large dead fuels as well as fine fuels (Bradshaw et al., 1983; Andrews et al., 2003). ERC(G) is commonly used for regional-scale calculations (Finney et al., 2011b). Due to the heavy weighting of large dead fuels, ERC(G) is mainly driven by weather conditions during the previous month and a half, which is the time it takes for dead woody debris 7.6-20.3 cm (3-8 inches) in diameter (also called 1000-hour fuels) to mostly equilibrate to constant ambient conditions (Fosberg et al., 1981).

ERC(G) has been shown to have a strong relationship with fire occurrence in Arizona: the probability of fire increases with ERC(G), and can be quantified with logistic regression (Andrews and Bevins, 2003; Andrews et al., 2003). Therefore, the ERC(G) is used by US federal land agencies both operationally (Predictive Services) and in simulation models that predict fire size and probability, including FSPro and FSim (Finney et al., 2011a; Finney et al., 2011b). However, the parameters of the logistic regression relating ERC(G) and fire occurrence vary with location, suggesting that fires are likely to ignite at different ERC(G) values in different areas due to variations in climate and fuels. For example, fuels tend to burn at a much lower (moister) ERC(G) on Washington's Olympic Peninsula, where relative humidity is higher and temperatures are lower during fire season, than in the Great Basin, where relative humidity is lower and temperatures are higher. Thus, ERC(G) should be regarded as a relative index; current ERC(G) values must be compared to historic values in the same location, as well as local fire occurrence information, in order to interpret them correctly (Schlobohm and Brain, 2002).

Associating fire occurrence and weather data

Each fire's location was assigned to the latitude/longitude of the centroid of its perimeter, and the discovery date was used as a proxy for ignition date. For each fire, we identified the closest pixel of weather data, in both space and time. For monthly indices (PPT, PDSI, and all SPIs), we queried the spatially closest pixel during the month of the fire's discovery. Values of monthly indices are based on conditions at the end of each month. We queried the daily ERC(G) data to identify the ERC(G) of the closest pixel on the fire's discovery date, as well as the six following days, and averaged these seven daily ERC(G) values. In the absence of data on containment dates and daily fire progression, we assumed that these first seven days were critical to fire spread. This assumption may not always hold true, since some large fires, especially those ignited by lightning under moderate conditions, may grow slowly for a period of weeks until a weather event spurs their growth. However, we were hesitant to use an analysis window longer than seven days for ERC(G) since this would increase the chance of erroneously incorporating low ERC(G) values associated with weather events that curtailed fire growth.

Statistical analyses

Empirical distributions of indices for fire vs. all conditions

The empirical frequency distributions of indices vary. For example, the SPI is normally distributed and centered at zero, with more than two-thirds of values between -1 and 1, indicating relatively normal conditions. Therefore, if fires occurred at random with respect to this index, from a purely probabilistic standpoint, fires would be more likely to occur at values close to zero than at extreme values of the index, simply because mild values occur more often by an order of magnitude. The same is true for PDSI: PDSI values signifying mild drought also occur much more frequently than extreme values. This property of PDSI may be why some studies have found that synchronous fires tend to occur at PDSI values signifying mild (frequently occurring) rather than extreme (rarely occurring) drought (e.g., Baisan and Swetnam, 1990; Hessl et al., 2004).

To remove the confounding effect of different empirical distributions in relation to fire occurrence, we tested whether the distribution of each index was significantly different during conditions under which large fires occurred than under all conditions, using two tests based on

the empirical frequency distribution (EFD) and the empirical cumulative distribution function (ECDF). To determine the empirical frequency distribution (EFD) of each index's values, we queried the gridded index data and created a histogram of all pixel values occurring during the study period from 1 January 1984 through 31 December 2008. We used all days of the year rather than attempt to delineate a fire season, since the length of fire season varies spatially across the western US and temporally from year to year. We then created histograms of index values associated with large fire events. For each index, to test whether the means of the two EFDs ("fire" vs. "all") were different, we compared the bootstrapped means of the two EFDs, using 500 random samples of n=1000 with replacement, and then constructed a 90% confidence interval around the means. Because many of the empirical distributions are non-normal, this bootstrapping approach was needed to create a confidence interval around the mean. We chose a sample size of 1000 in order to rectify bias introduced by extremely large (n>1,000,000 for "all" conditions) and unequal (n=5976 for "fire" conditions) population sizes.

Second, we plotted the empirical cumulative distribution function (ECDF) of each index for all values and statistically compared it to values associated with large fires. The null hypothesis was that the two distributions were the same. Because smaller values of PPT, PDSI, and SPI indicate drier conditions, the alternative hypothesis we tested was that the ECDF of the metric associated with large fires was greater than that of all values of the metric (if the ECDF is greater, the distribution is shifted to the left, suggesting lower index values). Conversely, higher values of ERC(G) indicate drier conditions, so the alternative hypothesis is that the ECDF of the "fire" distribution is less than that of "all" conditions (in this case, if the ECDF is less, the distribution is shifted to the right, signifying higher index values). The non-parametric test statistic D measures the maximum separation distance between the two distributions. As D increases, so does the likelihood that the two distributions are from different populations. The Kolmogorov-Smirnov (KS) test was applied to determine the probability that D occurred by chance. Due again to large and unequal sample sizes, we ran the KS test for 500 samples of n = 1000 for each index. We then calculated how many times the null hypothesis would have been rejected at alpha = 0.1 in order to determine whether the "fire" and "all" ECDFs were different. This methodology removes the confounding effect of the different frequency distributions of the indices, and determines whether each metric has power in detecting conditions conducive to large fire events.

Correlations of metrics with large fire occurrence

In order to remove confounding effects introduced by the distribution of the metric and by variations in microclimate, we converted weather and climate data to percentile-based measures that convey the relative rarity of a given index value for each microclimate/pixel. Thus, we focused on departure from median precipitation conditions as a metric for severity of dry or wet conditions, as measured by a suite of drought and fire-danger indices, rather than attempting to find a definition of drought that applies to all climates in the western US.

For each pixel where a fire occurred, we queried all values that occurred during the period of study. These were then sorted, in order to establish the rank of the index's value during each fire. Ranks were calculated based on the index values as a single pool for all seasons, all months, and all years. Ranks were then converted to percentiles. For PDSI, SPIs, and PPT, low percentiles (near zero) indicate extremely dry conditions, while high percentiles (near 100) indicate wet conditions. For ERC(G), the reverse is true: low percentiles (near zero) indicate fuels with high moisture content, while high percentiles (near 100) indicate dry fuels. Each fire was thus assigned a percentile for each index. For example, if the value of PPT for March 1997 ranked 100th of 200 values, signifying average conditions, the PPT percentile would be 50. Because each pixel has a different distribution of weather data, we found index percentiles for each individual pixel (therefore, an ERC(G) value of 57 may indicate 95th percentile conditions in one cell, while in another cell the 95th percentile ERC(G) value may be 89 – but in both cases the 95th percentile value indicates a comparable level of aridity for that microclimate). This methodology is similar to that of Alley (1984), who recommended a similar rank-based approach.

For each metric separately, we summed area burned and number of fires across the western US, binning fires by percentile class (e.g. 1st percentile, 2nd percentile). For example, if there were three fires that occurred during 100th percentile ERC(G) conditions (a 1000-ha fire that occurred in June 2000 in Arizona, a 1200-ha fire during August 2003 in Montana, and a 1500-ha fire in southern California in November 2008) then the total area burned during 100th percentile ERC(G) conditions would be 3700 ha. Essentially, the output is a histogram of area burned with 100 bins where each drought/precipitation percentile corresponds to a bin. The relationship of index percentiles to total area burned was then quantified using linear regression,

and evaluated by means of regression analysis (R^2) and tests of significance (p-values). Note that these correlations are based on index values during time periods when a fire occurred. The same methodology was repeated to produce linear models relating number of fires to index percentiles.

Results

Empirical distributions of indices for "fire" vs. "all" conditions

Empirical frequency distributions (EFDs) of drought indices are varied, and include bimodal, normal, and right-skewed (Figure 3). The EFD of PDSI is bimodal, due to the fact that the index value is reset at the end of a drought or pluvial episode, resulting in a dip in the frequency of the metric at values near zero (Palmer, 1965). Mild to moderate PDSI values (-2 to +2) occur most frequently in our dataset, with extreme values (e.g. -5 or +5) occurring very rarely, indicating the rarity of extreme drought and wet conditions as recorded by this index (Figure 3). Based on visual inspection of the graph, the distribution of PDSIs associated with large fire occurrence is shifted slightly to the left of the distribution of all PDSIs, indicating that fires tend to occur during lower PDSIs. The PDSI values most commonly associated with large fires are -0.5 to -2, indicating mild drought. The fact that most fires occur at values of PDSI indicating mild drought does not necessarily imply that mild drought is more conducive to large fire than extreme drought; rather, values of the index near zero occur much more frequently, meaning there is a relatively small number of months during which fires could potentially occur at rare extreme values of the index. This result also illustrates that extreme drought that cumulates over prolonged period of moisture deficit is not a prerequisite for fire occurrence. Instead, the proclivity for fire occurrence during mild drought conditions as assessed by the PDSI, may explain why years of fire synchrony tend to occur during years of mild-moderate rather than extreme drought simply because mild droughts occur much more frequently (Baisan and Swetnam, 1990; Balling et al., 1992; Swetnam and Betancourt, 1998; Westerling et al., 2003; Hessl et al., 2004; Heyerdahl et al., 2008a).

The EFD of ERC(G) is characterized by frequent occurrence of moderate ERC(G) values, while high values indicating extremely dry conditions are rare (Figure 3). Zero values occur most frequently (zero is assigned to indicate snow or high fuel moistures that preclude burning). The distribution of ERC(G) values associated with large fire events is visibly different

from that of ERC(G)s as a whole, being skewed toward the higher ERC(G) values typically associated with dry fuels.

In contrast to PDSI and ERC(G), the EFD of monthly precipitation values (PPT), in millimeters, is heavily right-skewed, with the lowest precipitation values being most common (Figure 3). The distribution of PPT during large fires events is more heavily skewed toward low PPTs than the distribution of PPT during the entire period of study, indicating fire events take place preferentially at lower PPTs.

The EFD of the Standard Precipitation Index is by definition normal due to its calculation, as discussed previously (Figure 3). The distribution of SPI3 values under which large fires ignite is shifted toward more negative (drier) values of SPI3 than that of the distribution of the metric as a whole, indicating that large fires do tend to burn more frequently under values of SPI3 that indicate drought. However, visual inspection of these figures indicates that this shift weakens as the period tabulated by the metric lengthens, until it is not visible for SPI24 (Figure 3).

We also performed quantitative testing of the means of the EFDs. Testing of the means indicated that the mean values of ERC(G), PPT, and SPI3 associated with large fires are significantly drier than the mean of all values at the 90% confidence level (Figure 4, Table 2). Confidence intervals of the means of the "fire" and "all" values distributions for PDSI, SPI6, SPI9, SPI12, and SPI24 overlapped, indicating that the means are not significantly different.

A second method for testing whether the distributions of fire and all conditions are different used the Kolmogorov-Smirnov test of the D statistic of the empirical cumulative distribution functions (ECDFs; Table 2). These Kolmogorov-Smirnov tests indicated that the "fire" distributions of ERC(G) and PPT are significantly different than the distributions of these metrics under all conditions, and strong evidence existed for SPI3 as well (Figure 5; Table 2). Evidence that the "fire" distributions of SPI6, SPI9, SPI12, and SPI24 are different from "all" conditions weakened as the time period tabulated by the metric increased (Table 2; Figure 5). For PDSI, relatively weak evidence exists that the two distributions are different, and this hypothesis would be rejected by both testing of the means (Figure 4) and approximately one-third of Kolmogorov-Smirnov statistic tests at alpha=0.1 (Figure 5; Table 2). Thus, PDSI is not strongly related to large fire occurrence.

Taken as a whole, these results suggest that shorter-term indices (ERC(G), PPT, and SPI3) are more strongly associated with large fire occurrence than longer-term metrics (PDSI, SPI6, SPI9, SPI12, and SPI24).

Correlations of metrics with large fire occurrence

The area burned by individual fires was not strongly related to raw index values. Results are shown for ERC(G) and PDSI, with the pattern being similar for the other metrics (Figure 6). The largest fires occur at frequent values of indices (moderate ERC(G), low PPT, moderate PDSI, and moderate SPI), rather than the most extreme values. For example, the largest fires did not occur at the highest ERC(G)s, which are rare in the record. Large fires occurred more often during the drier phase of the metrics (higher ERC(G)s, negative PDSI, and negative SPI); this relationship with SPI is stronger in the shorter phase of this metric (SPI3), and weakens progressively as the duration of the metric becomes longer. In the case of ERC(G), PPT, and PDSI, the relationship with fire area is further obscured by the fact that these metrics vary regionally (e.g. a precipitation value of 20 mm in a month may signify wet conditions in the Great Basin and dry conditions on the Washington Coast). However, by transforming indices to percentile values for each fire, the relationships become more apparent. For example, a scatterplot of ERC(G) percentile versus fire size illustrates that large fires tend to occur when ERC(G) is above the 80^{th} percentile (Figure 7).

We parameterized linear models relating index percentile to number of large fires (Table 3, Figure 8) and area burned (Table 4, Figure 9). Correlations between index percentile and number of large fires were stronger than those between index percentile and area burned for all metrics. ERC(G) percentile demonstrated the strongest relationship with area burned (adjusted R^2 =0.92; Table 4; Figure 9) as well as number of fires (adjusted R^2 = 0.94; Figure 8; Table 3). Number of fires and area burned increased exponentially with ERC(G) percentile. PPT percentile (Figure 8 and 9) demonstrated almost as strong a relationship with number of fires and area burned as ERC(G) (for number of fires, adjusted R^2 = 0.93; for area burned, adjusted R^2 =0.89). SPI3 percentile (Figure 8 and 9) had a strong correlation with number of fires (adjusted R^2 = 0.83) and moderate correlation with area burned (adjusted R^2 = 0.70). For SPI6, 9, 12, and 24 percentile (Figure 9), the models explained less than half of the variability in area burned, indicating a weak relationship between area burned and these indices. PDSI percentile also

showed a weak relationship with area burned (adjusted R^2=0.34, Figure 9), except perhaps at extremely low PDSI values (0-30th percentile), where area burned increases with drought severity. In addition, PDSI percentile had a weak relationship with number of large fires (adjusted R^2 = 0.30). Correlations with number of fires were somewhat stronger, with models explaining more than half the variability in the data for SPI6, 9, and 12 percentile, declining with the time period measured by the index. Based on these results, we concluded that ERC(G) percentile is the index with the most power in predicting large fire occurrence across the western US, followed closely by PPT percentile.

Discussion

We found strong correlations between fire occurrence (defined as total area burned and total number of fires) and certain drought/fire danger indices across the western US, indicating that models based on a single metric can account for over 90% of the variability in area burned across a large region, once metrics have been normalized to account for local climate. We therefore concluded that our methodology was successful in reducing the effect of confounding factors discussed in the background section, by: 1) accounting for the empirical distribution of indices by normalizing metrics to percentile, 2) removing the relative meanings of some indices by normalizing them to local climate, 3) using a consistent georeferenced dataset for fire occurrence provided by MTBS, which reduced problematic fire records, and 4) utilizing gridded index data to more closely represent weather and climate conditions near remote fire locations than datasets with coarser resolutions.

Once metrics were normalized to percentile, we found that metrics based on the previous 1-3 months of weather data had strong correlations with both total area burned and number of large fires, indicating that this time period is critical to producing the conditions conducive to large fires. As the time period tabulated by the metric lengthened, the relationship weakened. This result indicates the importance of dead fuel moisture in promoting or retarding the spread of large fires. Dead surface fuels (grass, litter, duff, and woody debris) are the primary carrier of surface fires, and provide the intensity necessary for surface fires to transition to crown fires (Van Wagner, 1977). Fine fuels such as grass are frequently referred to as 1-hour fuels, because they mostly equilibrate to constant ambient conditions within a few hours, while woody debris 7.6-20.3 cm (3-8 inches) in diameter falls into the 1000-hr category, meaning they take

approximately 40 days to mostly equilibrate with constant environmental conditions (Fosberg et al., 1981). Dead fuel moistures therefore largely depend on weather conditions within the previous month and a half. It follows, therefore, that monthly precipitation totals (PPT), which were strongly related to area burned and number of fires in the western US, are a major driver of dead fuel moisture values. Because ERC(G) contains fuels of all size classes, including a heavy weighting of 1000-hour fuels (Bradshaw et al., 1983; Andrews et al., 2003), this index also captures trends in fuel moistures largely based on weather during the previous month and a half. ERC(G) has two other properties which likely caused it to have a stronger relationship with fire occurrence than other indices in this study. First, ERC(G) calculation includes relative humidity and solar radiation terms, which are important determinants of fuel moisture and vegetation curing. As vegetation cures, it becomes more readily available to burn and thus contribute to increased fire intensity and rate of spread (Scott and Burgan, 2005). Second, ERC(G) is calculated on a daily timestep and can capture timing of precipitation events, which affect the potential for fires to grow. Of the indices analyzed, only ERC(G) captures daily weather, since other indices are summed over monthly intervals. However, ERC(G) calculation is more complex than that of PPT, which performed nearly as well, indicating that PPT could be used in situations where time, processing power, or data inputs are limited. SPI3 did not perform as well as ERC(G) or PPT, but was strongly correlated with number of large fires and moderately correlated with area burned in the western US. Given that SPI3 is based on precipitation during a 3-month period, we expect that it would have a moderately strong relationship with fuel moistures.

Indices based on longer timeframes had weaker or no relationship with fire occurrence. This result was likely due to the fact that longer-term indices do not strongly reflect recent precipitation and thus have weaker relationships with dead fuel moistures. For example, because PDSI is autoregressive, summer PDSI values will reflect antecedent conditions and are affected by winter/spring precipitation. Similarly, SPI9 for October-June could have an equivalent value for a 9-month period encompassing a dry October-March followed by a wet April-June, as it would for a wet October-March followed by a dry April-June. However, the effect on dead fuel moistures as well as the amount of vegetation that has cured would be extremely different.

The weather conditions surrounding the extensive 1910 fires in Montana and Idaho demonstrate a case where shorter-term metrics would have likely been more strongly correlated

with fire occurrence than longer-term metrics. In a 1931 study, the year 1910 was not listed as being among the 10 driest years for either state during the period of record (for Montana, 1895-1930, and for Idaho, 1898-1930) (Henry, 1931). Henry (1931) notes that, "The dry year 1910 is seemingly in a class by itself," with the onset of the drought being "quite sudden as compared with the others." Work by Brown and Abatzoglou (2010) using gridded weather data reinforces these conclusions: an anomalously wet and cool winter was followed by an anomalously dry and warm spring and summer. In the case of 1910, an infamous year of synchronous fires, longer-term metrics such as PDSI, SPI9, 12, or 24 would likely not have captured the conditions that promoted fire, while shorter-term metrics such as ERC(G) or PPT likely would have (Chuck McHugh, personal communication).

While shorter-term fluctuations in precipitation strongly affect dead fuel moistures, longer-term periods of dry weather affect live fuels. As noted above, long periods of dry weather may result in mortality and/or curing of some live fuels, increasing rates of spread and fire intensity (Scott and Burgan, 2005). This dynamic occurs seasonally in many ecosystems, but longer-than-average dry periods contribute to additional mortality. In addition, long droughts may reduce live fuel moisture of trees, which likely contributes to crown fire potential. However, live fuel flammability is still not well understood, with current research focusing on differences between new and old foliage and the abundance of flammable compounds, which fluctuate in response to seasonal drivers (Matt Jolly, personal communication). Metrics capturing longer time periods may relate in some way to these factors, but further research is needed to measure seasonal fluctuations in live fuel moistures and link them to index values.

Fire suppression has likely affected the relationship of fire occurrence with fuel conditions. Some evidence indicates that the relationship of PDSI and fire occurrence was stronger during the pre-suppression era (Miller et al., 2012), when fires may have burned under more moderate conditions. Current fire management policies in the western US tend to eliminate fires that can be suppressed, with suppression more effective under mild and moderate conditions (Finney et al., 2009), leaving fires that escape suppression under the most extreme weather conditions to burn most of the acreage. There are exceptions, including fires that are allowed to burn in remote areas under mild or moderate conditions. Suppression forces can often take advantage of small precipitation events to control or contain fires, with such precipitation events being captured by ERC(G) calculation. In the pre-suppression era, fires might have continued to

grow once these precipitation events ended. Prior to European colonization, Native American burning was also common in the US, with many tribes choosing to ignite burns during mild weather conditions in the spring (Lewis, 1973; Riley, 2001). MTBS data do not contain information on suppression efforts, therefore, it could not be included in our analysis. More research is needed to investigate how suppression affects the relationship between fire occurrence and drought.

We found stronger correlations between index percentiles and number of large fires than with area burned. We conclude short-term drought is a stronger driver of number of large fires than of total area burned, since probability of ignition increases with drier fuel moistures, while the area burned by large fires is also affected by other factors responsible for fire growth, including wind, temperature, topography, barriers to spread, fuel type, availability of fine fuels in some ecoregions, suppression tactics, and maturity of forest in stand-replacing regimes. We note that individual fire sizes were not strongly related to drought and fire danger indices, likely due to the effect of these factors. It is noteworthy, however, that precipitation indices showed a strong correlation with fire occurrence without including these other factors in statistical models.

Conclusions

The primary goals of this study were to: 1) investigate how shorter- and longer-term drought are related to fire occurrence in the western US by evaluating the strength of the correlation of various drought and fire danger indices with area burned and number of large fires, and 2) determine whether a single drought/fire danger index is strongly related to fire occurrence across the western US, since such a metric could be used in predictive modeling of large fires in current fire danger applications, fire history studies, and studies predicting future fire occurrence under changing climatic conditions. When converted to a percentile-based measure indicating departure from local median conditions, short-term metrics ERC(G) and monthly precipitation (PPT) had strong correlations with area burned ($R^2 = 0.92$ and 0.89 respectively) and number of large fires ($R^2 = 0.94$ and 0.93 respectively) in the western US over the study period (1984-2008). As the temporal scale of indices increased, the strength of their relationship with fire occurrence decreased. A likely reason for this result is that shorter-term metrics are more strongly related to dead fuel moistures, which are largely dependent on weather during the past

1-3 months. Longer-term metrics are not as sensitive to recent precipitation events that affect fuel moistures and thus fire occurrence. Although PDSI is the most commonly used drought metric in fire history studies and in efforts to predict area burned, we found that it is not strongly correlated with area burned ($R^2 = 0.34$ for PDSI percentile) or number of large fires ($R^2 = 0.30$), likely due to the fact that it is not strongly related to dead fuel moistures. We therefore recommend the use of ERC(G) or the more easily calculated PPT for use in applications that associate precipitation and fire occurrence.

Because ERC(G) and PPT are largely based on weather conditions during the previous month, they cannot be used for long-lead forecasting of fire occurrence, nor can we see a way that they could be calculated for use in fire history studies, which necessarily rely on annual tree-ring data. Little is currently known about the mechanisms that drive drought, especially during fire seasons, with precipitation anomalies associated with El Niño-Southern Oscillation (ENSO) being more strongly linked to winter than summer precipitation across much of the western US (Ropelewski and Halpert, 1986; McCabe and Dettinger, 1999). Hence, long-lead forecasting of fire danger is currently challenging, given our result that fire season precipitation is the strongest predictor of fire occurrence. However, if it were possible to predict synoptic patterns that cause negative precipitation anomalies that endure for more than a month, areas of high fire danger could in turn be predicted using forecast ERC(G) and PPT values.

Acknowledgements

Karin Riley appreciates financial support from the Jerry O'Neal National Park Service Student Fellowship. This study was also funded in part by the USFS Rocky Mountain Research Station and Western Wildland Environmental Threat Center. Our thanks to Rebecca Bendick and three anonymous reviewers for constructive critiques of this article. Kari Pabst and Jennifer Lecker of the Monitoring Trends in Burn Severity Project gave support regarding MTBS data. We thank Chuck McHugh for information on the 1910 fires.

References

Abatzoglou, J.T., 2011. Development of gridded surface meteorological data for ecological applications and modelling. International Journal of Climatology, doi: 10.1002/joc.3413.

Abatzoglou, J.T., Kolden, C.A., 2011. Relative importance of weather and climate on wildfire growth in interior Alaska. International Journal of Wildland Fire, 20(4), 479-486.

Ager, A.A., Vaillant, N.M., Finney, M.A., 2010. A comparison of landscape fuel treatment strategies to mitigate wildland fire risk in the urban interface and preserve old forest structure. Forest Ecology and Management, 259(8), 1556-1570.

Alley, W.M., 1984. The Palmer Drought Severity Index: limitations and assumptions. Journal of Climate and Applied Meteorology, 23, 1100-1109.

Andrews, P.L., 2005. Fire danger rating and fire behavior prediction in the United States, Proceedings of the Fifth National Research Institute of Fire and Disaster, Tokyo, Japan, pp. 106-118.

Andrews, P.L., Bevins, C.D., 2003. BehavePlus Fire modeling system, version 2: overview, Second International Wildland Fire Ecology and Fire Management Congress, Orlando, Florida.

Andrews, P.L., Loftsgaarden, D.O., Bradshaw, L.S., 2003. Evaluation of fire danger rating indexes using logistic regression and percentile analysis. International Journal of Wildland Fire, 12, 213-226.

Baisan, C.H., Swetnam, T.W., 1990. Fire history on a desert mountain range: Rincon Mountain Wilderness, Arizona, U.S.A. Canadian Journal of Forest Research, 20, 1559-1569.

Balling, R.C., Meyer, G.A., Wells, S.G., 1992. Relation of surface climate and burned area in Yellowstone National Park. Agricultural and Forest Meteorology, 60, 285-293.

Bradshaw, L.S., Deeming, J.E., Burgan, R.E., Cohen, J.D., 1983. The 1978 National Fire-Danger Rating System: technical documentation. US Department of Agriculture Forest Service, Intermountain Forest and Range Experiment Station General Technical Report INT-169, 44 pp.

Brown, T.J., Abatzoglou, J.T., 2010. The climate of the Big Blowup, Proceedings of the 3rd Fire Behavior and Fuels Conference. International Association of Wildland Fire, Birmingham, Alabama, USA, Spokane, Washington, USA.

Brown, T.J., Hall, B.L., Mohrle, C.R., Reinbold, H.J., 2002. Coarse assessment of federal wildland fire occurrence data. Report for the National Wildfire Coordinating Group. Desert Research Institute CEFA Report 02-04, 31 pp.

Calkin, D.E., Ager, A.A., Thompson, M.P., Finney, M.A., Lee, D.C., Quigley, T.M., McHugh, C.W., Riley, K.L., Gilbertson-Day, J.W., 2011. A comparative risk assessment framework for wildland fire management: the 2010 Cohesive Strategy Science Report. RMRS-GTR-262, 63 pp.

Cohen, J.D., Deeming, J.E., 1985. The National Fire Danger Rating System: basic equations. US Department of Agriculture Forest Service, Pacific Southwest Forest and Range Experiment Station General Technical Report PSW-82, 16 pp.

Collins, B.M., Omi, P.N., Chapman, P.L., 2006. Regional relationships between climate and wildfire-burned area in the Interior West, USA. Canadian Journal of Forest Research, 36, 699-709.

Dai, A., Trenberth, K.E., Qian, T., 2004. A global dataset of Palmer Drought Severity Index for 1870-2002: relationship with soil moisture and effects of surface warming. Journal of Hydrometeorology, 5, 1117-1130.
Daly, C., Neilson, R.P., Phillips, D.L., 1994a. A statistical-topographic model for mapping climatological precipitation over mountainous terrain. Journal of Applied Meteorology, 33, 140-158.
Daly, C., Neilson, R.P., Phillips, D.L., 1994b. A statistical-topographic model for mapping climatological precipitation over mountainous terrain. Journal of Applied Meteorology, 33(2), 140-158.
Eidenshink, J.C., Schwind, B., Brewer, K., Zhu, Z.-L., Quayle, B., Howard, S., 2007. A project for monitoring trends in burn severity. Fire Ecology, 3(1), 3-21.
Finney, M.A., Grenfell, I.C., McHugh, C.W., 2009. Modeling containment of large wildfires using generalized linear mixed-model analysis. Forest Science, 55(3), 249-255.
Finney, M.A., Grenfell, I.C., McHugh, C.W., Seli, R.C., Trethewey, D., Stratton, R.D., Brittain, S., 2011a. A method for ensemble wildland fire simulation. Environmental Modeling and Assessment, 16, 153-167.
Finney, M.A., McHugh, C.W., Grenfell, I.C., Riley, K.L., Short, K.C., 2011b. A simulation of probabilistic wildfire risk components for the continental United States. Stochastic Environmental Research and Risk Assessment, 25(7), 973-1000.
Fosberg, M.A., 1971. Climatological influences on moisture characteristics of dead fuel: theoretical analysis. Forest Science, 17, 64-72.
Fosberg, M.A., Rothermel, R.C., Andrews, P.L., 1981. Moisture content calculations for 1000-hour timelag fuels. Forest Science, 27(1), 19-26.
Guttman, N.B., 1998. Comparing the Palmer Drought Index and the Standardized Precipitation Index. Journal of the American Water Resources Association, 34(1), 113-121.
Guttman, N.B., Wallis, J.R., Hosking, J.R.M., 1992. Spatial comparability of the Palmer Drought Severity Index. Water Resources Bulletin, 28(6), 1111-1119.
Henry, A.J., 1931. The calendar year as a time unit in drought statistics. Monthly Weather Review, 59, 150-153.
Hessl, A.E., McKenzie, D., Schellhaas, R., 2004. Drought and Pacific Decadal Oscillation linked to fire occurrence in the inland Pacific Northwest. Ecological Applications, 14(2), 425-442.
Heyerdahl, E.K., Morgan, P., Riser II, J.P., 2008a. Multi-season climate synchronized historical fires in dry forests (1650-1900), Northern Rockies, USA. Ecology, 89(3), 705-716.
Heyerdahl, E.K., Morgan, P., Riser II, J.P., 2008b. Multi-season synchronized historical fires in dry forests (1650-1900), Northern Rockies, USA. Ecology, 89(3), 705-716.
Holden, Z.A., Crimmins, M.A., Cushman, S.A., Littell, J.S., 2011. Empirical modeling of spatial and temporal variation in warm season nocturnal air temperatures in two North Idaho mountain ranges, USA. Agricultural and Forest Meteorology, 151(261-269).
Kangas, R.S., Brown, T.J., 2007. Characteristics of US drought and pluvials from a high-resolution spatial dataset. International Journal of Climatology, 27(10), 1303-1325.
Karl, T.R., 1986. The sensitivity of the Palmer Drought Severity Index and Palmer's Z-Index to their calibration coefficients including potential evapotranspiration. Journal of Climate and Applied Meteorology, 25, 77-86.
Lewis, H.T., 1973. Patterns of Indian burning in California: ecology and ethnohistory. Ballena Press, Ramona, California, 101 pp.

Littell, J.S., McKenzie, D., Peterson, D.L., Westerling, A.L., 2009. Climate and wildfire area burned in western U.S. ecoprovinces, 1916-2003. Ecological Applications, 19(4), 1003-1021.
Lloyd-Hughes, B., Saunders, M.A., 2002. A drought climatology for Europe. International Journal of Climatology, 22, 1571-1592.
McCabe, G., Dettinger, M.D., 1999. Decadal variations in the strength of ENSO teleconnections with precipitation in the Western United States. International Journal of Climatology, 19, 1399-1410.
McKee, T.B., Doesken, N.J., Kleist, J., 1993. The relationship of drought frequency and duration to time scales, Eighth Conference on Applied Climatology, Anaheim, California.
Miller, J.D., Skinner, C.N., Safford, H.D., Knapp, E.E., Ramirez, C.M., 2012. Trends and causes of severity, size, and number of fires in northwestern California, USA. Ecological Applications, 22(1), 184-203.
Morgan, P., Heyerdahl, E.K., Gibson, C.E., 2008. Multi-season climate synchronized forest fires throughout the 20th century, Northern Rockies, USA. Ecology, 89(3), 717-728.
Omernik, J.M., 1987. Ecoregions of the conterminous United States. Annals of the Association of American Geographers, 77(1), 118-125.
Palmer, W.C., 1965. Meteorological drought. U.S. Department of Commerce Research Paper No. 45, 58 pp.
Preisler, H., Burgan, R.E., Eidenshink, J.C., Klaver, J.M., Klaver, R.W., 2009. Forecasting distributions of large federal-lands fires utilizing satellite and gridded weather information. International Journal of Wildland Fire, 18, 508-516.
Preisler, H., Westerling, A.L., 2007. Statistical models for forecasting monthly large wildfire events in western United States. Journal of Applied Meteorology and Climatology, 46, 1020-1030.
Riley, K.L., 2001. Forest, fire, home: experiences with wildfire in the Klamath Mountains of Northern California. Master's, Humboldt State University, Arcata, California, 542 pp.
Ropelewski, C.F., Halpert, M.S., 1986. North American precipitation and temperature patterns associated with the El Nino/Southern Oscillation (ENSO). Monthly Weather Review, 114, 2352-2362.
Rothermel, R.C., 1972. A mathematical model for predicting fire spread in wildland fuels. US Department of Agriculture Forest Service Research Paper INT-115, 40 pp.
Schlobohm, P., Brain, J., 2002. Gaining an understanding of the National Fire Danger Rating System. National Wildfire Coordinating Group PMS 932, NFES 2665, 72 pp.
Schmidt, K.M., Menakis, J.P., Hardy, C.C., Hann, W.J., Bunnell, D.L., 2002. Development of coarse-scale spatial data for wildland fire and fuel management. U.S. Department of Agriculture, Forest Service Rocky Mountain Research Station GTR-RMRS-87, 41 pp.
Scott, J.H., Burgan, R.E., 2005. Standard fire behavior fuel models: a comprehensive set for use with Rothermel's surface fire spread model. USDA Forest Service General Technical Report RMRS-GTR-153, 72 pp.
Sellers, W.D., 1965. Physical climatology. University of Chicago Press, Chicago, 272 pp.
Sheffield, J., Wood, E.F., Roderick, M.L., 2012. Little change in global drought over the past 60 years. Nature, 491, doi: 10.1038/nature11575.
Strauss, D., Bednar, L., Mees, R., 1989. Do one percent of forest fires cause ninety-nine percent of the damage? Forest Science, 35(2), 319-328.

Swetnam, T.W., Betancourt, J.L., 1998. Mesoscale disturbance and ecological response to decadal climate variability in the American Southwest. Journal of Climate, 11, 3128-3147.

Thornthwaite, C.W., 1948. An approach toward a rational classification of climate. Geographical Review, 38(1), 55-94.

Thornthwaite, C.W., 1953. Topoclimatology, Proceedings of Toronto Meteorological Conference. Royal Meteorological Society, Toronto, Canada, pp. 227-232.

Thornton, P.E., Thornton, M.M., Mayer, B.W., Wilhelmi, N., Wei, Y., Cook, R.B., 2012. Daily surface weather on a 1 km grid for North America. Oak Ridge National Laboratory Distributed Active Archive Center http:/daymet.ornl.gov/, doi: 10.3334/ORNLDAAC/Daymet_V2,

Trouet, V., Taylor, A.H., Carleton, A.M., Skinner, C.N., 2009. Interannual variations in fire weather, fire extent, and synoptic-scale circulation patterns in northern California and Oregon. Theoretical and Applied Climatology, 95, 349-360.

Van Wagner, C.E., 1977. Conditions for the start and spread of crown fire. Canadian Journal of Forest Research, 7, 23-34.

Westerling, A.L., Gershunov, A., Brown, T.J., Cayan, D.R., Dettinger, M.D., 2003. Climate and wildfire in the western United States. American Meteorological Society, DOI: 10.1175/BAMS-1184-1175-1595.

Westerling, A.L., Gershunov, A., Cayan, D.R., Barnett, T.P., 2002. Long lead statistical forecasting of area burned in western U.S. wildfires by ecosystem province. International Journal of Wildland Fire, 11, 257-266.

Westerling, A.L., Swetnam, T.W., 2003. Interannual to decadal drought and wildfire in the Western United States. Eos, Transactions, American Geophysical Union, 84(49), 545-560.

Figure 1. The study area was the western US, west of the grasslands of the Great Plains region, as delineated by Omernik ecoregion boundaries. This figure shows all fires included in the analysis, selected from the Monitoring Trends in Burn Severity database based on the following criteria: 1) fires with centroid inside the study area, and 2) greater than or equal to 404.7 ha (1000 ac) in size. Map projection: Albers.

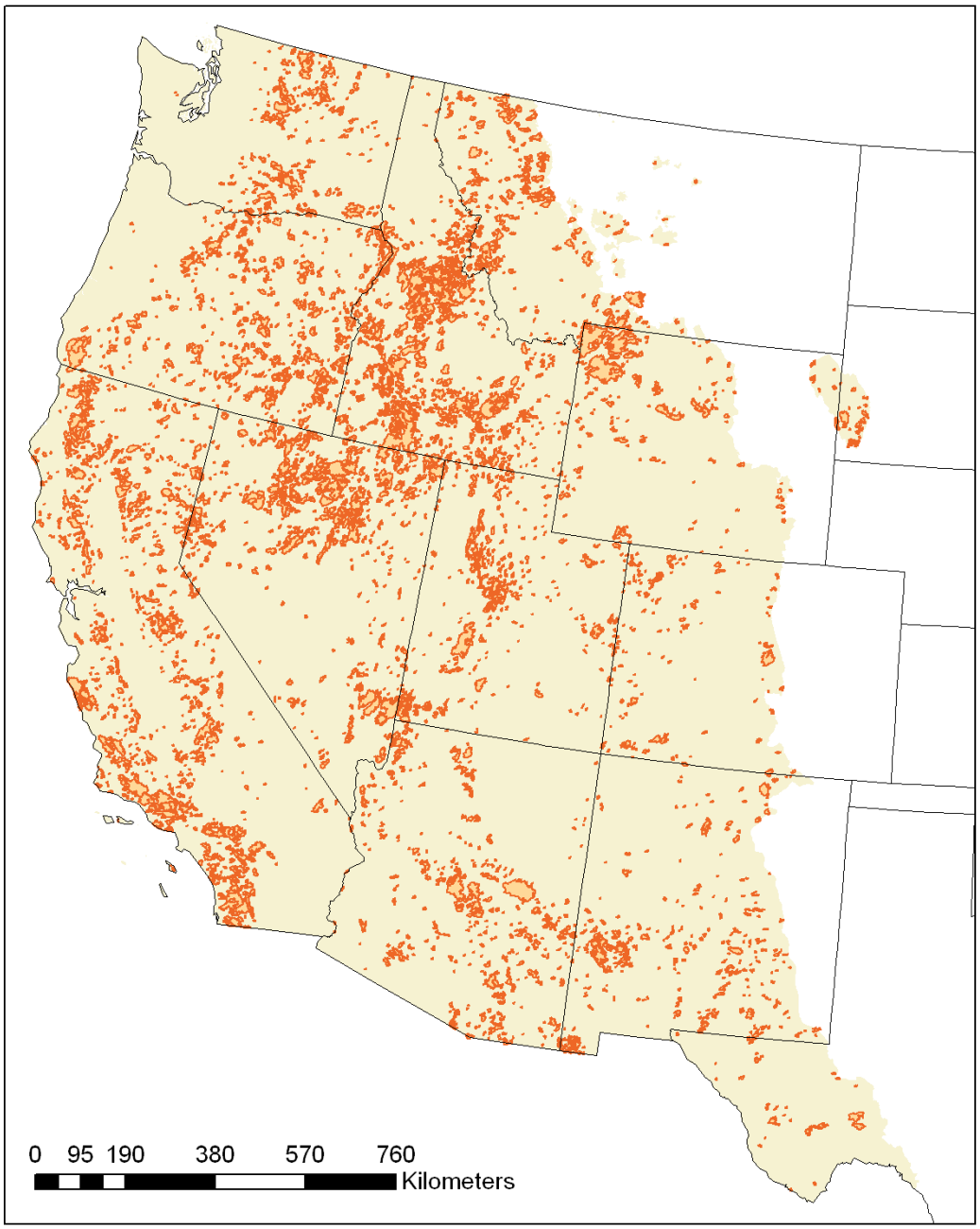

Figure 2. Gridded 3-month Standardized Precipitation Index (SPI3) data for June 2008, with US Climate Division boundaries, illustrating fine-scale variability in SPI3. Map projection: Albers.

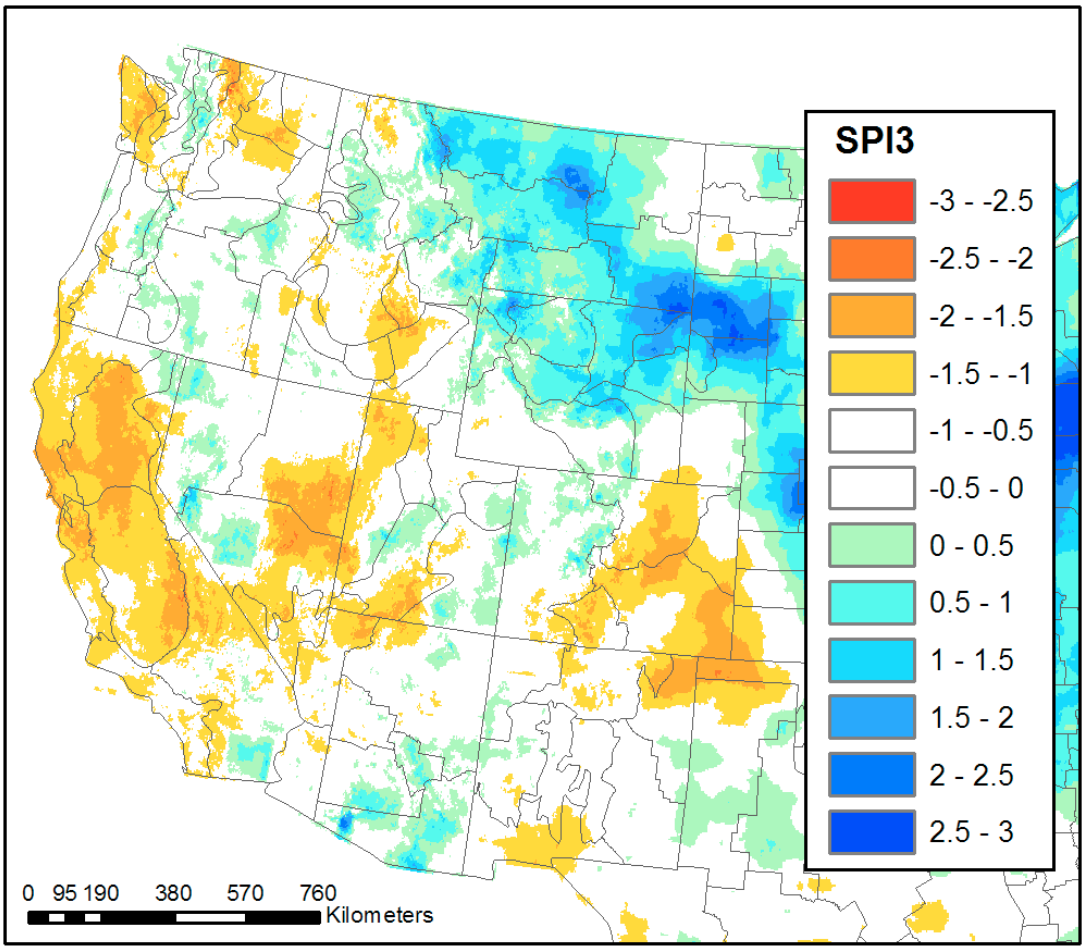

Figure 3. Empirical frequency distribution (EFD) of index values 1/1/1984 – 12/31/2008 in the study area (shown in black), plotted with EFD of index values associated with large fire events (shown in gray). Empirical frequency distribution of some indices is markedly different for fire events than as a whole, suggesting that these indices are related to fire occurrence. Units of PPT are given in millimeters.

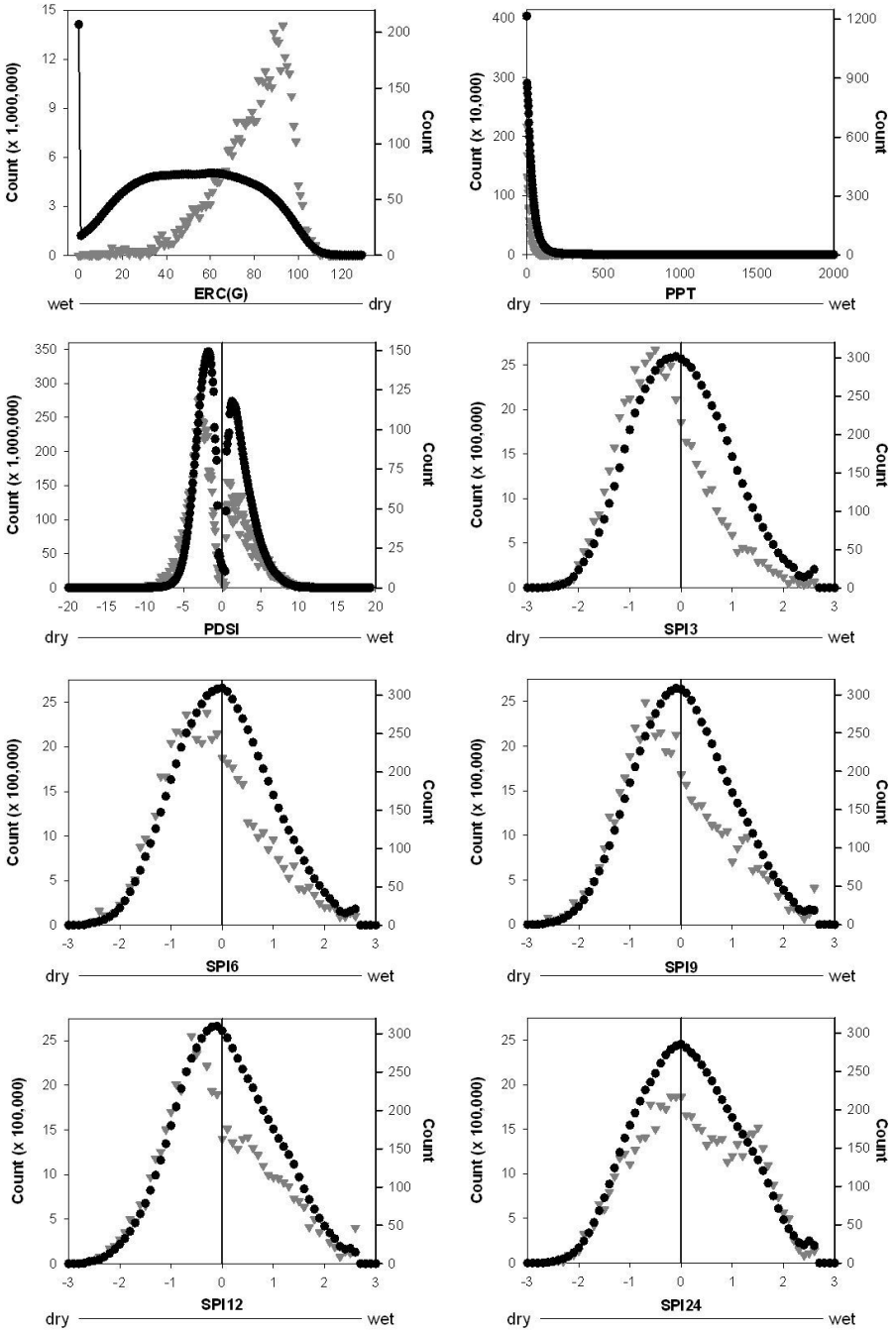

Figure 4. The 90% confidence interval around the mean value of indices, for all index values during 1/1/1984 – 12/31/2008 and for index values associated with large fires events. Bootstrapped mean was calculated on a sample with replacement, with sample size =1000, and sample conducted 500 times. Pairs of confidence intervals overlapped for PDSI, SPI6, SPI9, SPI12, and SPI24, meaning there is no statistical evidence that the means are different under conditions when large fires occurred.

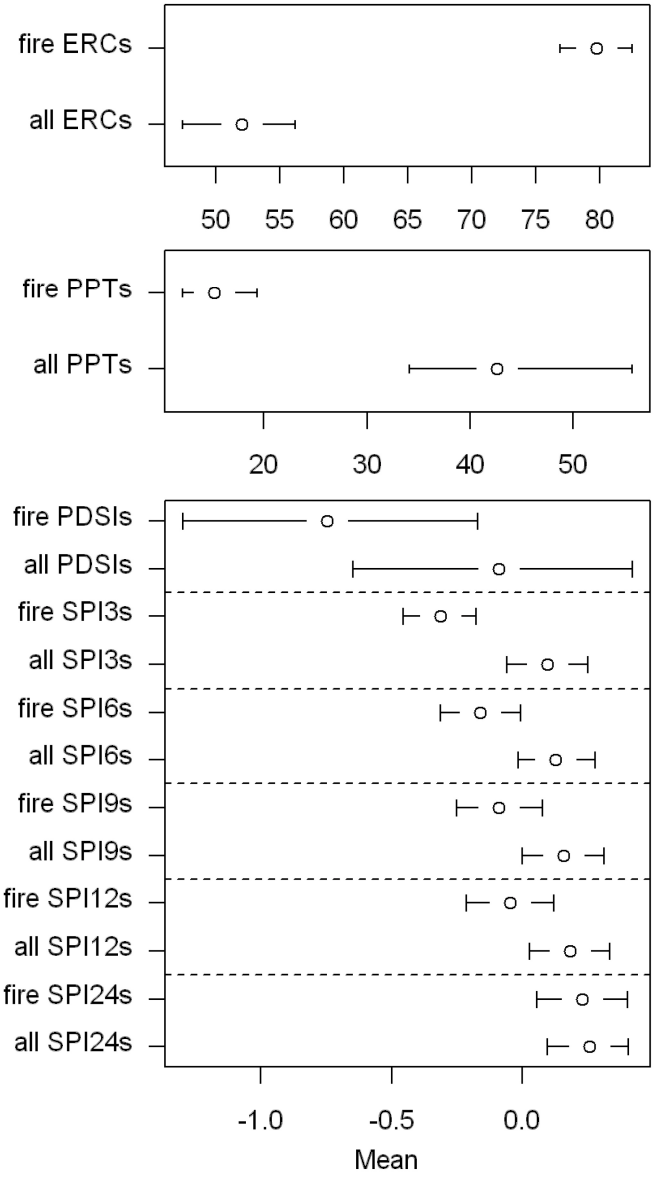

Figure 5. Empirical cumulative distribution functions of indices, for all conditions and those associated with fires. For fires, *n*=5976 (shown in gray). Due to processing limitations, 1,000,000 values were randomly sampled from the index values to create the ECDF of "all" values (shown in black). a) ERC(G) (7-day average), b) PPT, c) PDSI, d) SPI3, e) SPI6, f) SPI9, g) SPI12, h) SPI24.

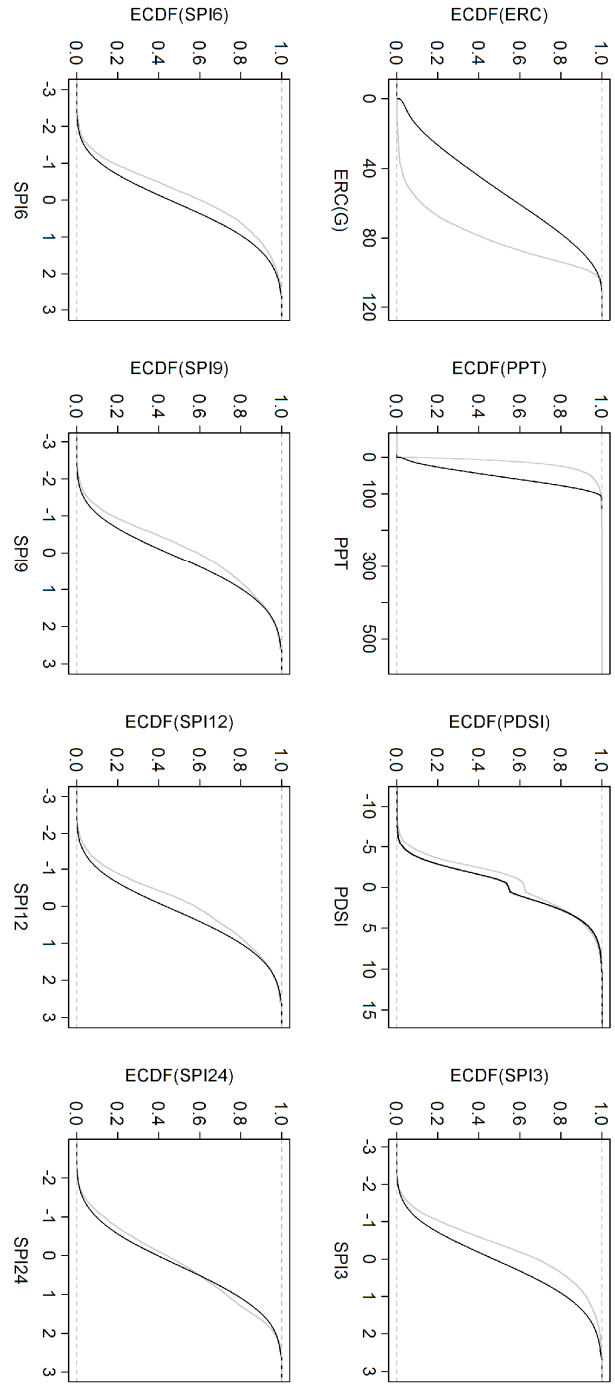

Figure 6. Fire area versus ERC(G) (left), and fire area versus PDSI (right).

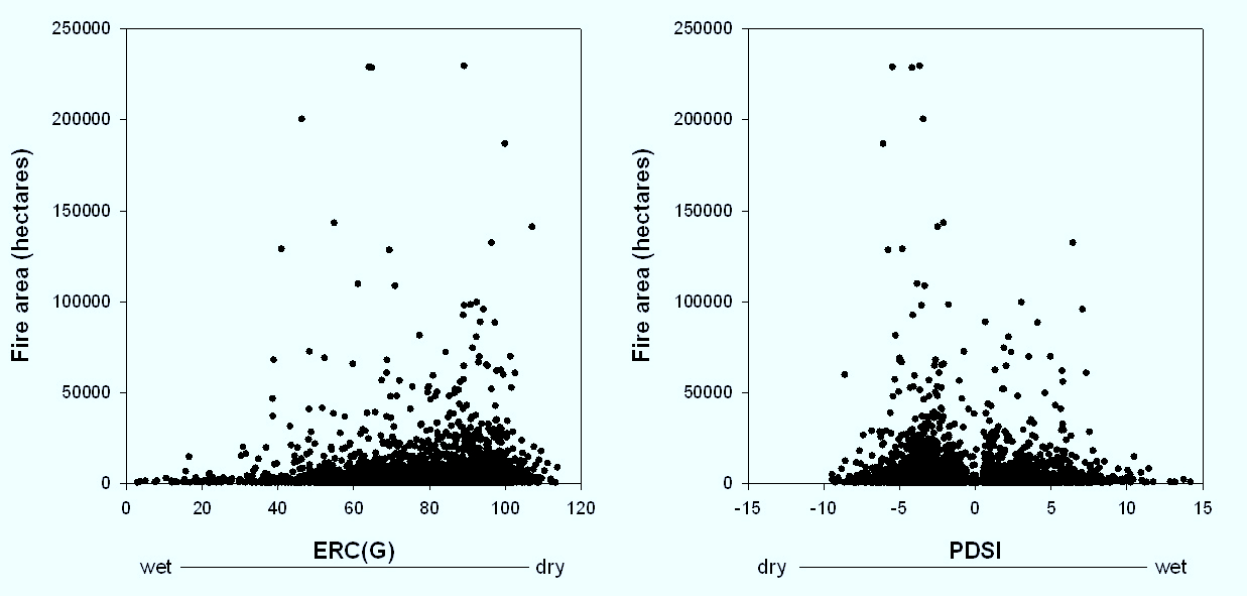

Figure 7. Fire area versus ERC(G) percentile.

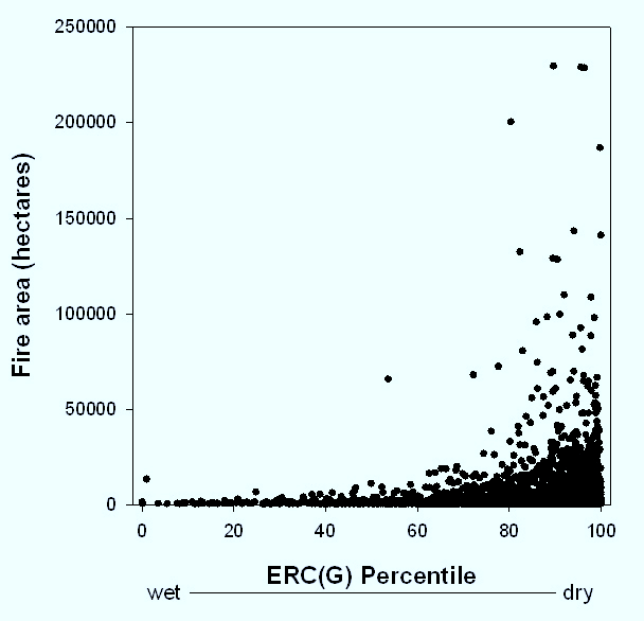

Figure 8. Total number of fires, summed by index percentile. Each point represents the total area burned in that percentile, with 100 percentile bins. a) ERC(G), b) PPT, c) PDSI, d) SPI3, e) SPI6, f) SPI9, g) SPI12, h) SPI24.

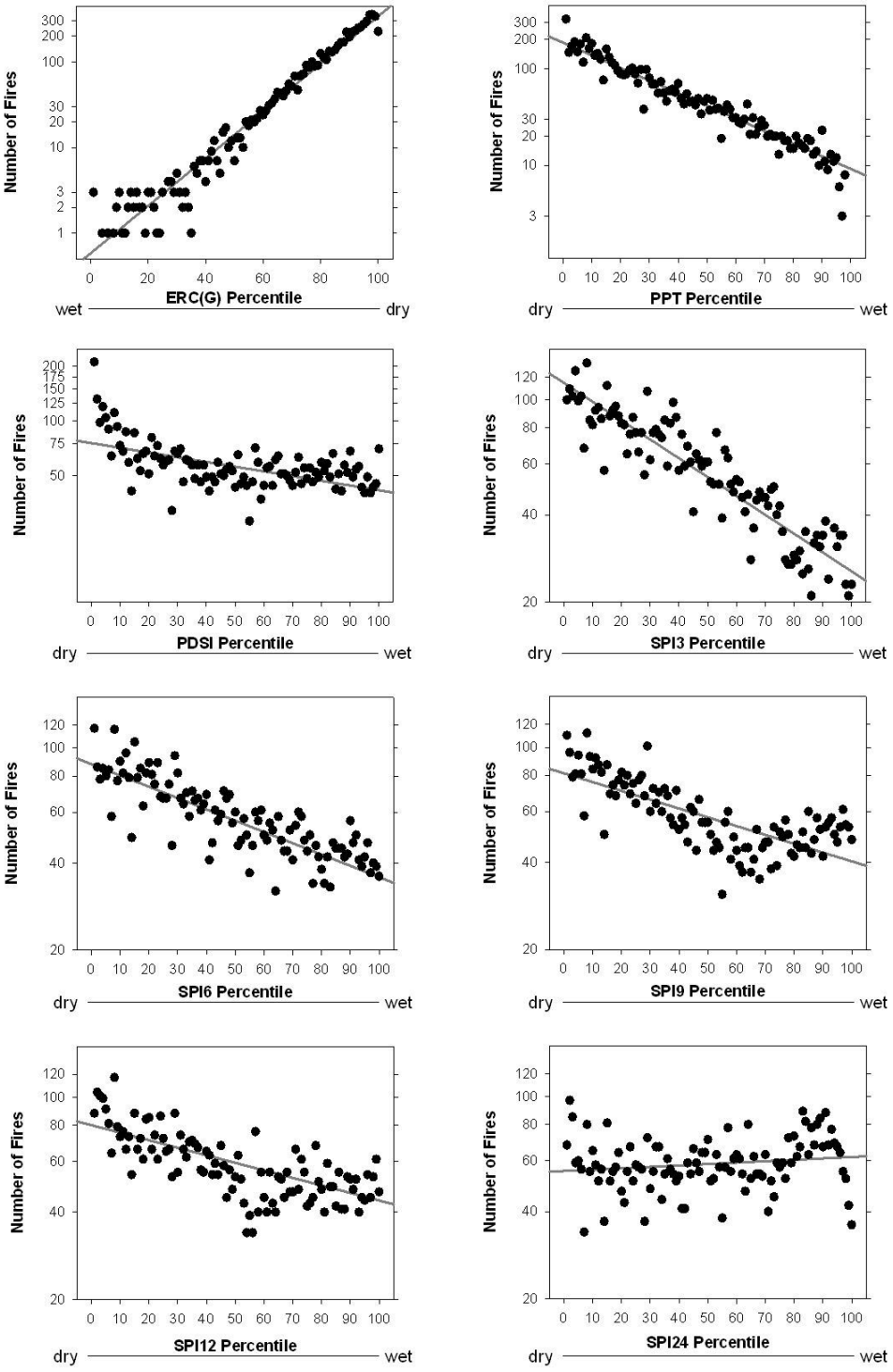

Figure 9. Sum of area burned, by index percentile. Each point represents the total area burned in that percentile, with 100 percentile bins. a) ERC(G), b) PPT, c) PDSI, d) SPI3, e) SPI6, f) SPI9, g) SPI12, h) SPI24.

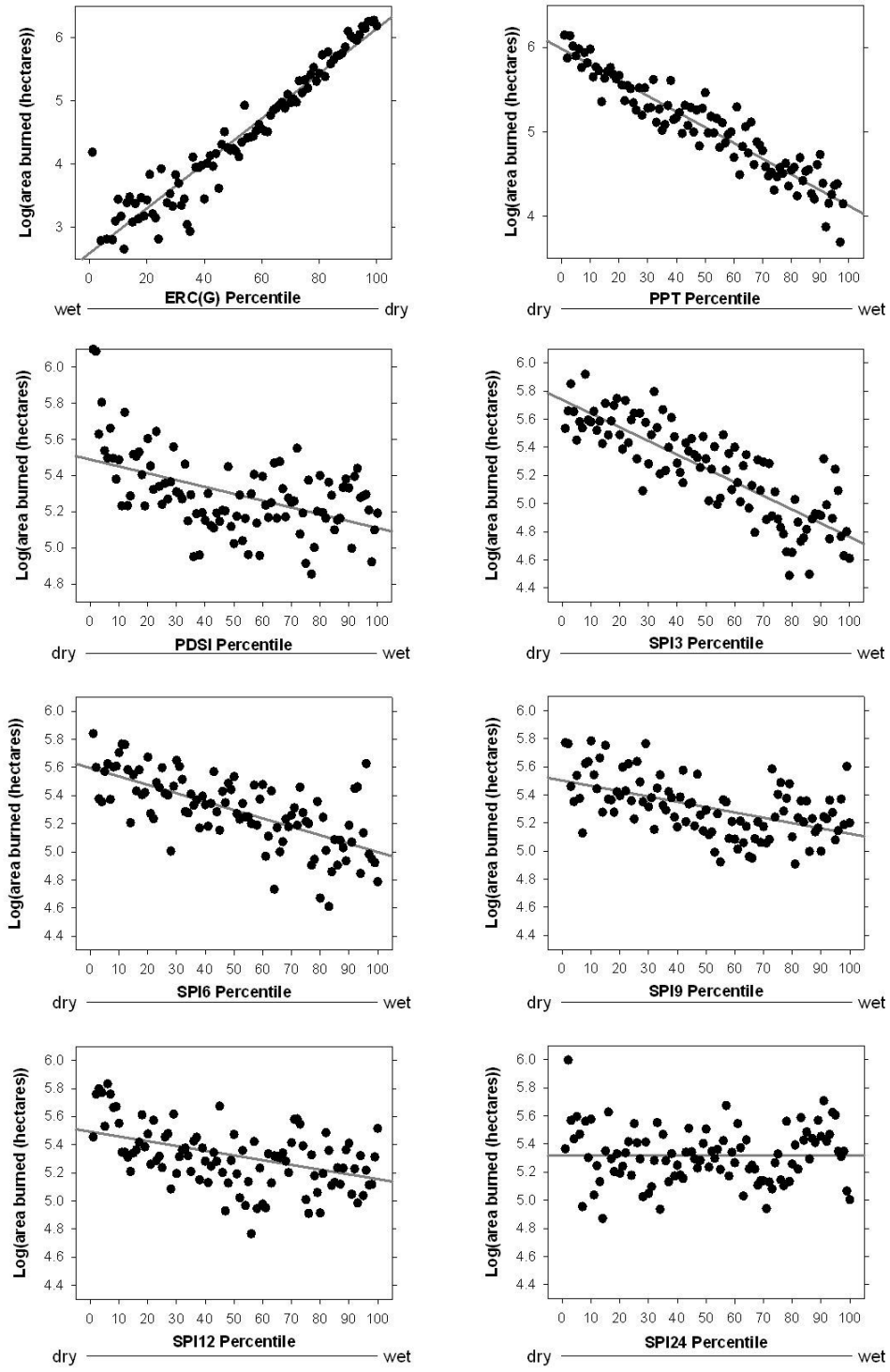

Table 1. Review of literature relating drought and precipitation indices calculated from weather records to area burned in the western US during the modern era. Studies utilize fire records kept by US Department of Interior National Park Service, Bureau of Land Management, Bureau of Indian Affairs, US Department of Agriculture Forest Service, states, and/or private landowners.

Region	Authors	Years	Statistic relating drought index to area burned
Yellowstone National Park	Balling *et al.* (1992)	1895-1990	Summer PDSI for two adjacent climate divisions. Pearson product-moment correlation (r) = -0.04 to -0.38
Interior Western US	Collins *et al.* (2006)	1926-2002	Average PDSI calculated for 3 regions (1=MT, ID, WY; 2=NV, UT; 3=AZ, NM) based on averaging PDSI value for each state. R^2 = 0.27 – 0.43 for current year; R^2 = 0.44 – 0.67 for model including current year and two previous years
Western US	Littell *et al.* (2009)	1916-2003 and 1980-2003	Forward selection regression used to parameterize generalized linear models based on seasonal precipitation, temperature, and PDSI for current and previous year; dependent variable was annual area burned by ecoprovince, R^2 = 0.33 – 0.87
National Forests in northwestern California	Miller *et al.* (2012)	1910-1959 and 1987-2008	Regression models predicted number of fires based on summer PDSI (June, July, and August) (R^2 = 0.37) and total annual area burned (R^2 = 0.37) for the first time period. For the later time period, total precipitation in June, July, and August was correlated with number of fires (R^2 = 0.60) and total annual area burned (R^2 = 0.54).
Idaho and western Montana, US	Morgan *et al.* (2008)	1900-2003	Spearman's rank correlation between annual area burned and climate-division temperature and precipitation. Summer precipitation: r = -0.49 Summer temperature (normalized): r = 0.59
Two National Forest groups in southern Oregon and northern California	Trouet *et al.* (2009)	1973-2005	National Forests clustered into 2 groups with similar temporal sequences of area burned. Daily ERC(G) was averaged to produce a seasonal value for July-August-September. Correlation (r) between annual area burned and seasonal ERC(G) = 0.32 – 0.4
US West	Westerling *et al.* (2003)	1980-2000	Monthly PDSI values are "the average of values interpolated from US climate divisions" onto a 1x1 degree grid. Pearson's correlation (r) ~ -0.7 – 0.8. (note: lagged positive correlations in arid regions may indicate abundant moisture for fine fuel growth)

Table 2. Statistics comparing empirical distributions of indices during large fire events with those during all conditions. The null hypothesis (H_o) was that the two distributions were the same. The alternative hypothesis (H_a) for PDSI, SPIs, and PPT was that the ECDFs of the index during fires is greater than that of all values; for ERC(G), H_a was that the ECDF of ERC(G) associated with fire events is less than that of all ERC(G)s. H_o was rejected a higher percentage of the time for shorter-term metrics (at alpha=0.1), constituting evidence that large fire occurrence is more strongly related to shorter-term metrics. The D statistic measures the maximum separation distance between the two distributions, with higher values suggesting higher likelihood that the two distributions are different.

Index	Median of means (fire)	Median of means (all)	Means different based on 90% CI?	D (median)	Percent of tests in which H_o rejected
ERC(G)	79.8	52.1	yes	0.52	100
PPT	15.1	42.6	yes	0.36	100
SPI3	-0.3	0.1	yes	0.26	95.5
SPI6	-0.2	0.1	no	0.2	78.6
SPI9	-0.1	0.2	no	0.2	77.8
SPI12	-0.05	0.2	no	0.19	72.6
PDSI	-0.7	-0.1	no	0.19	70
SPI24	0.23	0.26	no	0.11	18.6

Table 3. Linear models relating index percentiles to number of large fires.

Index	Model	R^2
ERC(G)	$Log_{10}N = 0.02768 * (ERC_{pct}) - 0.2333$	0.94
PPT	$Log_{10}N = -0.01389 * (PPT_{pct}) + 2.303$	0.93
PDSI	$Log_{10}N = -0.002438 * (PDSI_{pct}) + 1.878$	0.30
SPI3	$Log_{10}N = -0.006487 * (SPI3_{pct}) + 2.058$	0.83
SPI6	$Log_{10}N = -0.003710 * (SPI6_{pct}) + 1.944$	0.68
SPI9	$Log_{10}N = -0.002978 * (SPI9_{pct}) + 1.910$	0.52
SPI12	$Log_{10}N = -0.002813 * (SPI12_{pct}) + 1.903$	0.52
SPI24	$Log_{10}N = -0.000473 * (SPI24_{pct}) + 1.743$	0.012

Key to table:
A = area burned
N = number of large fires
ERC_pct = ERC(G) percentile
PPT_pct = PPT percentile
PDSI_pct = PDSI percentile
SPI3_pct = SPI3 percentile
SPI6_pct = SPI6 percentile
SPI9_pct = SPI9 percentile
SPI12_pct = SPI12 percentile
SPI24_pct = SPI24 percentile
R^2 = adjusted R^2 of model

Table 4. Linear models relating drought indices to area burned.

Index	Model	R^2
ERC(G)	$Log_{10} A = 0.03551 * (ERC_{pct}) + 2.592$	0.92
PPT	$Log_{10} A = -0.01862 * (PPT_{pct}) + 5.984$	0.89
PDSI	$Log_{10} A = -0.003780 * (PDSI_{pct}) + 5.4875$	0.25
SPI3	$Log_{10} A = -0.009755 * (SPI3_{pct}) + 5.738$	0.70
SPI6	$Log_{10} A = -0.005972 * (SPI6_{pct}) + 5.595$	0.46
SPI9	$Log_{10} A = -0.003784 * (SPI9_{pct}) + 5.502$	0.28
SPI12	$Log_{10} A = -0.003366 * (SPI12_{pct}) + 5.492$	0.23
SPI24	$Log_{10} A = 0.000007998 * (SPI24_{pct}) + 5.317$	-0.010

Key to table:
A = area burned
N = number of large fires
ERC_pct = ERC(G) percentile
PPT_pct = PPT percentile
PDSI_pct = PDSI percentile
SPI3_pct = SPI3 percentile
SPI6_pct = SPI6 percentile
SPI9_pct = SPI9 percentile
SPI12_pct = SPI12 percentile
SPI24_pct = SPI24 percentile
R^2 = adjusted R^2 of model

Chapter 4.

Conclusions

The two studies presented in this dissertation document illustrate two disparate approaches to statistical modeling of hazard and risk resulting from rare stochastic disturbance events. These two studies can be integrated to inform global and continental prediction. In this chapter, I briefly review conclusions of the studies, discuss similarities between them, and present some key insights.

Chapter 2 demonstrated that small post-fire debris flows occur with a higher relative frequency than non-fire-related debris flows. The empirical cumulative distribution function of post-fire debris flow volumes was composed of smaller events than that of non-fire-related debris flows. In addition, this study demonstrated for the first time that post-fire events follow a power-law distribution, but that the slope of this distribution was steeper than that of non-fire-related debris flows. These results suggest that fire produces a number of changes in vegetation and soil characteristics that produce a higher proportion of small debris flows, by increasing the proportional frequency of small events and/or producing debris flows in small zero-order drainages not susceptible to them under unburned conditions. These changes in vegetation and soil characteristics tend to increase overland flow, available sediment, and soil moisture, as well as decrease the strength of the regolith. In regions where sediment transport is supply-limited, wildfire likely provokes smaller debris flows by increasing their probability and frequency. Because the distribution of post-fire debris flows is different from that of non-fire-related debris flows, post-fire debris flows must be regarded as coming from a different population, with commensurate differences in driving factors. Unfortunately, because the two types of events are from different populations, what is known about non-fire-related debris flows (a much larger n), cannot be applied directly to statistical modeling of post-fire debris flows (a smaller n) without further investigation of these differences. Collection of magnitude information on more post-fire debris flows will be necessary to contribute to understanding of how changes in the post-fire environment are related to debris flow volume, and produce definitive statistical models for post-fire debris flows.

In Chapter 3, strong correlations were found between short-term drought/fire-danger indices and fire occurrence across the western US for the study period 1984-2008. Statistical models for Energy Release Component for fuel model G (ERC(G)) explained 92% of the variability in area burned and 94% of the variability in number of fires. Model performance for monthly precipitation (PPT) was almost as strong, explaining 93% of the variability in number of fires and 89% of the variability in area burned. Both of these metrics measure short-term precipitation, on the order of a month to a month and a half. As the time period measured by the metrics lengthened, correlations weakened. Notably, Palmer Drought Severity Index (PDSI), which has a timescale of approximately 2-9 months and is the most commonly used metric in studies relating drought to fire occurrence, had weak correlations with both area burned (R^2 = 0.34) and number of fires (R^2 = 0.3), suggesting it is not strongly related to fire occurrence across the western US during the period of study. The strong correlations between shorter-term indices and fire occurrence are likely related to strong associations between these indices and moisture content of dead surface fuels, which are the primary carrier of surface fires. This result suggests the utility of shorter-term rather than longer-term indices in fire danger applications.

In both studies, simple mathematical models accounted for variation in rare stochastic disturbance events at regional to global scales, suggesting the utility of such models for hazard prediction at these scales. This work contributed to understanding of factors influencing debris flows and large fires, as well as their impacts. Bringing together information and techniques from disparate fields, these studies provided an integrated understanding of hazard prediction for rare and/or stochastic events.

Additional key insights included:

- Advances in technology over the past few decades aided this work. These advances included: 1) handheld GPS units with a high degree of accuracy, which were used for mapping the perimeter of debris flow fans, 2) mapping of burns from remote sensing using satellite imagery, 3) gridded weather data with 4-8 km resolution, and 4) the ability of desktop computers to process large datasets resulting from the use of such data. These advances in technology allowed for higher precision in model inputs.
- Compilations of disturbance events were needed for statistical models. This research was aided by a new publicly available dataset, the Monitoring Trends in Burn Severity project, which records fire size, location, and date (Eidenshink et al., 2007). However,

debris flow magnitudes had to be compiled from the literature and original field work for this dissertation, with a comprehensive database presented as one of the results.

- Parameterization of hazard models for both post-fire debris flows and large fires would benefit from better records. Fire records in the US are not tracked by a single system, and when multiple systems are aggregated, duplicate records result. Debris flow events (at least those that are published in the scientific literature) have been studied and recorded primarily in certain areas (the Alps, North American Coast Ranges, and the Rockies), with other areas having little or no coverage (including Asia, Australia, and Africa).

In conclusion, prediction of the magnitude of a single rare stochastic disturbance event remains a challenge, but the statistical models presented in this dissertation contribute to hazard prediction at regional and global scales, as well as understanding of driving mechanisms. For debris flows, the frequency-magnitude distributions presented herein can be used to derive the relative probability of an event of a certain size, for non-fire-related debris flows at the global scale and for post-fire debris flows in the western US. In the case of fire occurrence, the analysis contributes to real-time identification of areas of high hazard in the western US using short-term drought/fire-danger indices.

References

Eidenshink, J.C., Schwind, B., Brewer, K., Zhu, Z.-L., Quayle, B., Howard, S., 2007. A project for monitoring trends in burn severity. Fire Ecology, 3(1), 3-21.